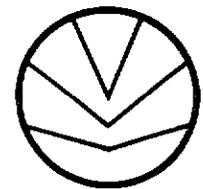# Simulation of Gas Condensate Reservoir Performance

Keith H. Coats,* SPE, Intercomp Resource Development and Engineering, Inc.

SPE 10512

Summary

This paper presents a generalized equation of state (EOS) that represents several widely used cubic EOS's. The generalized form is obtained by manipulation of Martin's EOS[1] and is applied in this study.

A component pseudoization procedure that preserves densities and viscosities of the pseudocomponents and the original mixture as functions of pressure and temperature is described. This procedure is applied with material balance requirements in generation of two-component, black-oil properties for gas condensates. Agreement between resulting black-oil and fully compositional simulations of gas condensate reservoir depletion is demonstrated for a very rich, near-critical condensate. Also, agreement between EOS compositional results and laboratory expansion data is shown.

The fully compositional simulation necessary for below-dewpoint cycling is performed for the near-critical condensate with a wide range of component pseudoizations. Results show the well-known necessity of splitting the C_{7+} fraction and indicate a minimal set of about six total components necessary for acceptable accuracy.

Introduction

Gas condensate reservoirs are simulated frequently with fully compositional models. This paper presents a pseudoization procedure that reduces the multicomponent condensate fluid to a pseudo two-component mixture of surface gas and oil. This allows the use of a simpler, less expensive, modified black-oil model that accounts for both gas dissolved in oil and oil vapor in the gas.

A major question in the use of the black-oil model is whether the two-component description can represent adequately the compositional phenomena active during the depletion or the cycling of gas condensate reservoirs. This question is especially pertinent to near-critical or very rich gas condensates. This paper, therefore, includes a comparison of black-oil and compositional simulations for depletion and below-dewpoint cycling of a naturally occurring, rich condensate only 15°F [8.3°C] above its critical temperature.

Like a number of unreported cases for leaner condensates, the two models give very similar results for depletion. In addition, the two models give identical results for cycling above dewpoint provided that certain conditions are satisfied. However, the black-oil model is not applicable to cycling below dewpoint, so results of the compositional model are compared for different multi- component descriptions to estimate the minimal number and identity of components necessary for acceptable accuracy.

The compositional calculations reported here use variants of the Redlich-Kwong[2-5] and Peng-Robinson[6] EOS's. This paper discusses a general cubic EOS form based on work by Martin[1] that encompasses all these EOS's. A general-component pseudoization procedure is presented, followed by its application to gas condensates. The black-oil PVT properties obtained and the agreement between laboratory test data and EOS calculated results are given for the rich condensate. Black-oil and compositional simulation results are then compared for depletion and below-dewpoint cycling of the condensate. Finally, the compositional-model cycling results are compared for different degrees of pseudoization (lumping) of components.

A General Form for Cubic EOS's

Use of an EOS in compositional simulation of reservoir performance and laboratory tests requires two basic equations that give the compressibility factor z and the fugacity of each component for a homogeneous mixture (phase). The two equations,

$$z = z(p, T, x) \qquad \text{.............................(1a)}$$

and

$$f_i = f_i(p, T, x), \quad i = 1, 2 \ldots n, \qquad \text{...............(1b)}$$

give these quantities as functions of pressure, temperature, and phase composition $x = \{x_i\}$.

A number of EOS's have been developed and are in wide use. These are the Redlich and Kwong[2] (RK*), modifications by Zudkevitch and Joffee[3] and Joffee et al.[4] (ZJRK) and by Soave[5] (SRK), and the Peng and Robinson[6] (PR) EOS.

Martin[1] shows that all cubic EOS's can be represented by a single general form. Use of Martin's work and basic thermodynamic relationships yields generalized forms for Eqs. 1a and 1b as follows:

$$z^3 + [(m_1 + m_2 - 1)B - 1]z^2 + [A + m_1 m_2 B^2$$

$$-(m_1 + m_2)B(B+1)]z - [AB + m_1 m_2 B^2(B+1)] = 0,$$

$$\text{.............................(2a)}$$

*Initials within parentheses denote the various EOS's.

and

$$\ln \Psi_i \equiv \ln \frac{f_i}{px_i} = -\ln(z-B)$$

$$+ \frac{A}{(m_1-m_2)B}\left(\frac{2\sum\limits_{j=1}^{n} A_{ij}x_j}{A}\right.$$

$$\left. -\frac{B_i}{B}\right) \ln \frac{z+m_2B}{z+m_1B} + \frac{B_i}{B}(z-1), \quad \ldots \ldots \ldots \ldots (2b)$$

where

$$A= \sum_{j=1}^{n} \sum_{k=1}^{n} x_j x_k A_{jk}, \quad \ldots \ldots \ldots \ldots \ldots \ldots (3a)$$

$$B= \sum_{j=1}^{n} x_j B_j, \quad \ldots \ldots \ldots \ldots \ldots \ldots \ldots \ldots (3b)$$

$$A_{jk} =(1-\delta_{jk})(A_jA_k)^{0.5}, \quad \ldots \ldots \ldots \ldots \ldots (3c)$$

$$B_j = \Omega_{bj}p_{rj}/T_{rj}, \quad \ldots \ldots \ldots \ldots \ldots \ldots \ldots (3d)$$

and

$$A_j = \Omega_{aj}p_{rj}/T_{rj}^2. \quad \ldots \ldots \ldots \ldots \ldots \ldots \ldots (3e)$$

The δ_{jk} are binary interaction coefficients, symmetric in j and k with $\delta_{jj}=0$. For the RK, SRK, and ZJRK equations, $m_1=0$ and $m_2=1$. For the PR equation, $m_1 =1+\sqrt{2}$ and $m_2 = 1-\sqrt{2}$.

Eqs. 2a and 2b stem from the manipulation of Martin's results. Their general form is useful in minimizing the volume of code necessary (in compositional models or PVT programs) to represent different EOS's. Further details of the derivation of Eqs. 2a and 2b are given in Appendix A.

As discussed by the authors of the various equations, the Ω_a and Ω_b appearing in Eqs. 2a through 3e are theoretically universal constants, Ω_a^o and Ω_b^o, determined when the EOS is forced to satisfy the van der Waals conditions: $(dp/dv)_T$ and $(d^2p/dv^2)_T=0$ at the critical point. In practice, however, the Ω_a and Ω_b values are treated generally as component-dependent functions of temperature, $\Omega_{ai}(T)$ and $\Omega_{bi}(T)$, as follows:

$$\text{RK: } \Omega_{bi} = \Omega_b^o \text{ and } \Omega_{ai}=\Omega_a^o/T_{ri}^{0.5},$$

$$\text{SRK: } \Omega_{bi} = \Omega_b^o \text{ and } \Omega_{ai}=\Omega_a^o[1+(0.48+1.574\omega_i$$

$$-0.176\omega_i^2)(1-T_{ri}^{0.5})]^2,$$

$$\text{ZJRK: } \Omega_{bi} = \Omega_{bi}(T) \text{ and } \Omega_{ai}=\Omega_{ai}(T),$$

and

$$\text{PR: } \Omega_{bi} = \Omega_b^o \text{ and } \Omega_{ai}=\Omega_a^o[1+(0.37464$$

$$+1.54226\omega_i -0.26992\omega_i^2)(1-T_{ri}^{0.5})]^2.$$

The Ω_a^o and Ω_b^o values follow:

	Ω_a^o	Ω_b^o
RK, SRK, and ZJRK:	0.4274802	0.08664035
PR:	0.457235529	0.077796074

The ZJRK equation determines $\Omega_{ai}(T)$ and $\Omega_{bi}(T)$ for a given component, i, at a given temperature, T, below critical so that component vapor pressure and saturated liquid density at T are matched exactly.[3,4]

Eqs. 2a and 2b are used in conjunction with the Newton-Raphson techniques described by Fussell and Yanosik[7] in the PVT and compositional models (described below) to perform saturation pressure and flash calculations.

Pseudoization

The term pseudoization denotes the reduction in the number of components used in EOS calculations for reservoir fluids. Pseudoization is important in reservoir calculations because of the large number of real components (e.g., in C_{7+} fraction) in reservoir fluids. Compositional model computing times can increase significantly with the number of components used.

We can think of pseudoization in terms of either lumping components or combining streams. Consider a homogeneous mixture of n components of composition $\{z_i\}$, denoted simply as mixture z. Mixture z can be divided into m ($m<n$) mixtures or streams $x^1, x^2 \ldots x^m$ so that $z=\Sigma\alpha_\ell x^\ell$—i.e.,

$$z_i = \sum_{\ell=1}^{m} \alpha_\ell x_i^\ell, \quad \ldots \ldots \ldots \ldots \ldots \ldots \ldots (4)$$

where

$$\sum_{i=1}^{n} x_i^\ell =1.0, \quad \ldots \ldots \ldots \ldots \ldots \ldots \ldots (5)$$

and

$$\sum_{\ell=1}^{m} \alpha_\ell =1.0. \quad \ldots \ldots \ldots \ldots \ldots \ldots \ldots (6)$$

The mixtures x^ℓ are pseudocomponents, normalized by Eq. 5, and α_ℓ is the mol fraction of Pseudocomponent x^ℓ in Mixture z. The Mixture z might be flashed at a low pressure and temperature with liquid and gas separator products resulting. Therefore, the two components, x^1 =separator gas and x^2 =separator liquid, represent two pseudocomponents satisfying Eq. 4, obtained by a combination of streams. With some oversimplification, this is the basis of the black-oil treatment that has been used
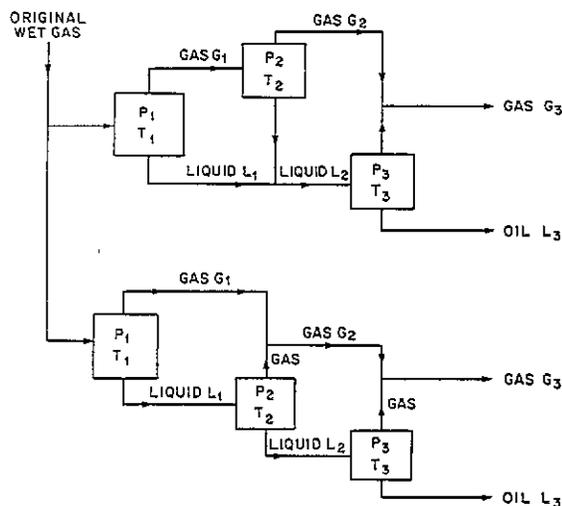
Fig. 1—Examples of gas condensate separation yielding two components—oil and gas.

for decades. Each of these two pseudocomponents includes some of each of the n components present in the original mixture.

In lumping components, each pseudocomponent consists of a subset of the original n components, and none of the members of this subset are present in any of the other pseudocomponents. For example, a Mixture z of $n=8$ components, CO_2, C_1, C_2, C_3, C_4, C_5, C_6, and C_{7+}, might be pseudoized to $m=5$ pseudocomponents, $x^1 = C_1$, $\{x^2 = CO_2, C_2\}$, $\{x^3 = C_3, C_4\}$, $\{x^4 = C_5, C_6\}$, and $x^5 = C_{7+}$.

This pseudoization procedure does not demonstrate how the pseudocomponents are defined or obtained, nor does it relate in any way to the two-phase behavior of the Mixture z or any of the pseudocomponents. The procedure assumes that m pseudocomponent definitions or compositions, x^ℓ, are given and are obtained from some original n-component Mixture z. The procedure determines pseudocomponent properties (e.g., p_c, T_c, Ω_a, and Ω_b) and pseudocomponent binary interaction coefficients so that two conditions are satisfied for all pressures and temperatures.

1. EOS calculations will yield identical density (z-factor) and viscosity for each pseudocomponent whether performed in a single-component mode or in an n-component mode.

2. For all mixtures of the m pseudocomponents (including the original mixture, z), the EOS calculations will yield identical mixture density and viscosity whether performed in an m-pseudocomponent mode or in an n-component mode.

Appendix B gives the equations defining pseudocomponent critical properties, Ω_a, Ω_b, and pseudobinary interaction coefficients that satisfy these conditions.

The usefulness of this pseudoization procedure is shown in two cases. First, in CO_2 or solvent flooding calculations where direct contact miscibility is assumed, the injected CO_2 mixture or solvent and the original reservoir oil composition can be pseudoized to pseudocomponents 1 and 2. The compositional model can be run then in a two-component mode with the EOS (and viscosity correlation), giving density and viscosity variation vs. pressure and composition identical to that obtained in a full

n-component calculation. A power law can be substituted for viscosity, and dispersion control or extension, similar to the work of Koval,[8] can be introduced. Equivalence of this two-component and full n-component simulations requires that original reservoir oil composition be uniform and that injected solvent composition be constant for all time.

A second case is cycling above dewpoint or depletion of a gas condensate reservoir. This case is described in detail in the following sections.

Pseudoization of a Gas Condensate Fluid

A gas condensate reservoir originally above dewpoint pressure is discussed and procedural steps are outlined briefly. The calculations are described in detail in Appendix C and are illustrated in connection with real fluids in sections below. First a stand-alone, EOS PVT program is used to match laboratory PVT data, usually including dewpoint pressure, expansion tests at reservoir temperature, and surface separation data. The EOS is then used to flash the original reservoir fluid through desired single- or multistage surface separation (Fig. 1). The gas and liquid n-component Compositions G_3 and L_3 are selected as pseudocomponents 1 and 2—gas and liquid or oil. This EOS flash gives n-component compositions, molecular weights, and densities at final-stage separator conditions of the two pseudocomponents, gas and oil, which are used in the modified black-oil model. Thus the black-oil model production expressed as stock-tank barrels of oil and standard cubic feet of gas can be converted to mols or mass of each of the n components in the original reservoir fluid. The two pseudocomponent properties are calculated as described in Appendix B.

Appendix C shows that the PVT program performs a constant-composition or constant-volume expansion to calculate a two-component or black-oil PVT table of B_o, R_s, μ_o, c_o, and r_s as single-valued functions of pressure at reservoir temperature. The table omits B_g and μ_g because they are obtained from the EOS in pseudo two-component mode in the black-oil simulator. The reason for omission is that B_g and μ_g are not single-valued functions of pressure in cycling calculations; rather, they depend on composition and pressure. Pseudo two-component properties required by the EOS and viscosity-correlation calculations in the black-oil simulator are generated by the PVT program and are read as input data to the simulator.

This procedure (Appendix C) differs in several respects from a calculation of black-oil properties for volatile oils or condensates given recently by Whitson and Torp.[9] We have not calculated differences in black-oil PVT curves yielded by the two approaches nor determined the effect of any such differences on black-oil model results.

For cycling above dewpoint, the black-oil simulator reproduces gas density and viscosity variation with pressure and composition identical to that obtained in an n-component compositional model simulation, subject to two conditions. The reservoir originally must contain an undersaturated (above dewpoint) gas condensate of uniform composition, and injected (or cycling lean) gas must be the surface separation gas, defined as pseudocomponent 1. If injected-gas composition does not equal that of the surface-separation gas, results of the black-oil and full-compositional models will differ.

For depletion below dewpoint pressure, we have found close agreement between gas deliverability and instantaneous oil/gas producing ratios calculated by the two-component black-oil and n-component compositional simulations. This has occurred for a number of condensates ranging from very lean to near-critical and extremely rich. Essentially, this agreement reflects the fact, noted by Jacoby and Yarborough[10] and Fussell,[11] that composition has a negligible effect on K values for depletion of gas condensates. Jacoby and Yarborough used laboratory test data, while Fussell used laboratory data in field-scale, single-well, compositional simulation of depletion.

For cycling below dewpoint, the two-component simulation gives results (e.g., C_{5+} recovery vs. time) that can be quite inaccurate, especially for rich condensates as illustrated below. The inapplicability of two-component calculations to below-dewpoint cycling reflects the findings of Cook et al.[12] They showed that accuracy of calculated vaporization during gas cycling of volatile oils requires that the C_{7+} fraction be split into a number of fractions. In addition, Fussell and Yarborough[13] showed that cycling results in a significant composition dependence of K values and that composition dependence cannot be obtained from volumetric (expansion) test data alone.

Description of Models

This PVT program is a general-purpose, stand-alone program coded to use any of the RK, SRK, ZJRK, or PR EOS's. However, we will describe only those features pertinent to its use in this paper. The program includes a nonlinear regression calculation that performs an automatic adjustment of EOS parameters to match a variety of laboratory PVT measurements. The regression variables are specified by the user and may be any subset of the EOS parameters. These parameters are Ω_{ai}^o and Ω_{bi}^o for each of the n components and the $n(n-1)/2$ binary interaction coefficients. We will denote the regression variable set selected in a given case by $\{v_i\}$, $i=1, 2 \ldots I$.

The data to be matched in a single regression may include any number of sample compositions at the same or different specified temperatures. For each sample, data entered may include (1) saturation pressure, (2) densities of equilibrium gas and oil at saturation pressure, (3) K values at that pressure, (4) constant composition, constant volume, and/or differential expansion data, including volume percent liquid, gas and oil densities, and K values at each expansion pressure, and (5) multistage separation data, including GOR, gas and oil densities, and K values for each stage. The set of all nonzero data entered is denoted by $\{d_j\}$, $j=1, 2 \ldots J$.

The regression is a nonlinear programming calculation that places default or user-specified upper and lower limits on each regression variable v_i. Subject to these limits, the regression determines values of v_i that minimize the objective function F.

$$F= \sum_{j=1}^{J} W_j \left| d_j-d_j{}^c \right| \div d_j, \quad \ldots \ldots \ldots \ldots \ldots (7)$$

where d_j^c and d_j are calculated and observed values of observation j. The term W_j is a weight factor, internally set or specified by the user. Default values are 1.0 for most data but are 40 for saturation pressure and 20 for

primary-phase (oil for an oil sample, gas for a condensate) density at saturation pressure.

The program regresses on condensate data, determines two pseudocomponents from specified surface separation conditions, and calculates pseudocomponent EOS parameters and the two-component black-oil PVT table (Appendix C). The results are stored in a data file in a format acceptable to the black-oil simulator.

The program allows a splitting of a sample plus fraction (e.g., C_{7+}) into a number of extended fractions. This calculation is a slight modification of a probabilistic model presented by Whitson.[14] He demonstrates excellent agreement between data and his model's calculation of the extended analysis given by Hoffmann et al.[15]

Within a single execution, the program can perform, in sequence, splitting of the plus fraction; regression with the resulting n-component representation; user-specified pseudoization—grouping or lumping—to n_1 components ($n_1 < n$); repeat of regression with n_1 components; pseudoization to $n_2 (< n_1)$ components; repeat of regression, etc. Calculations of expansions or other tests, with printed comparisons of calculated vs. observed data, can be interspersed in this sequence along with storage in a data file of EOS parameters in a format acceptable to the compositional simulator.

Extended fraction (C_7 through C_{40}) properties (p_c, T_c, M, T_B, etc.) are stored internally, as shown by Whitson.[14] Whitson's values are modified somewhat from values given by Katz and Firoozabadi.[16]

The black-oil model used here is a fully implicit, three-dimensional, three-phase model described previously[17] that accounts both for oil in the gas phase and for gas dissolved in the oil phase as functions of pressure, thereby allowing gas condensate or oil reservoir simulation. In the condensate case, the model calculates B_g and μ_g from an EOS to allow dependence on composition and pressure in cycling calculations.

The compositional model used in this work is an altered version of an implicit model described previously.[18] That model has been extended to use any of the four EOS's mentioned in this work and an IMPES formulation.

Condensate Reservoir Depletion Applications

Rich-Gas Condensate A. Table 1 lists data for the naturally occurring rich-gas Condensate A with bottomhole and recombined sample dewpoints of 3,025 and 3,115 psia [20 857 and 21 477 kPa] at the 325°F [163°C] reservoir temperature. Single-stage separation data at 624.7 psia [4307 kPa] and 100°F [38°C] give a liquid content of 586 bbl/MMscf [3.29×10^{-3} m³/std m³]. This fluid is close to critical because the critical temperature was 310°F [154°C]. Liquid yield for the three-stage separation of Table 1 is 347.4 STB/MMscf [46.2 dm³/kmol] at 14.7 psia [101.4 kPa] and 60°F [15.6°C].

Complete definition of a set of Condensate A compositional results requires a description of the EOS used, the regression data set, the regression variable set, information on whether the bottomhole or recombined sample composition was used, and the number and definitions of components used. The results (Figs. 2 through 5) were obtained from the ZJRK EOS for the bottomhole sample. The regression data set information is included in Table 2.

TABLE 1—RICH-GAS CONDENSATE A DATA AT 325°F

	Bottomhole Sample	Recombined Sample	C_{7+} Properties
Dewpoint (psia)	3,025	3,115	Specific gravity = 0.8044
Mol Fraction CO_2	0.0226	0.0201	Molecular weight = 148
N_2	0.0567	0.0562	
C_1	0.4574	0.4679	
C_2	0.1147	0.1265	
C_3	0.0759	0.0587	
C_4	0.0638	0.0604	
C_5	0.0431	0.0392	
C_6	0.0592	0.0478	
C_{7+}	0.1066	0.1232	

Three-Stage Separation (Recombined Sample)

Stage	p (psia)	T (°F)	GOR (scf/bbl)	Gas Gravity	Liquid Gravity	Liquid Molecular Weight	Liquid Shrinkage
1	624.7	100	1706.9	0.762	—	80.62	
2	94.7	80	297.8	0.997	—	—	0.8920
3	14.7	75	260.6	1.78	0.738	—	0.8447

Constant Composition Expansions at 325°F
(Bottomhole Sample)

p (psia)	Relative Volume	Liquid Volume (%)	Gas z Factor
9,255	0.6990		1.6695
8,000	0.7190		1.4851
7,000	0.7419		1.3407
6,000	0.7718		1.1956
5,000	0.8132		1.0497
4,000	0.8771		0.9058
3,025*	1.0000	0.0	0.7810
3,015	1.0028	29.95	
3,005	1.0060		
2,995	1.0093	32.59	
2,970	1.0157	33.49	
2,950	1.0221	33.40	
2,900	1.0350	33.26	
2,800	1.0672	32.49	
2,205	1.3235	27.21	
1,835	1.5834	21.23	
1,490	1.9703	15.77	
1,165	2.6179		

Recombined Sample

Point	p (psia)	Relative Volume	Liquid Volume (%)	Gas z Factor
1	9,255	0.6943		1.6625
2	8,000	0.7169		1.4724
3	7,000	0.7411		1.3319
4	6,000	0.7725		1.1900
5	5,000	0.8163		1.0479
6	4,422	0.8523		1.9676
7	3,115*	1.0000	0.0	0.7998
8	3,100	1.0036	10.0	
9	3,075	1.0092	21.7	
10	3,060	1.0132	25.4	
11	3,030	1.0213	28.8	
12	3,017	1.0253	29.9	
13	2,992	1.0334	30.8	
14	2,905	1.0575	32.0	
15	2,775	1.0978	31.6	
16	2,660	1.1381	30.2	
17	2,555	1.1784	28.9	
18	2,385	1.2592	26.6	
19	1,980	1.5017	21.2	
20	1,792	1.6576	18.6	

Gas gravities relative to air = 1.0.
Liquid gravities relative to water = 1.0.
Gas standard volumes at 14.7 psia, 60°F.
*Dewpoint.

The four regression variables were Ω_a^o and Ω_b^o of methane and C_{7+}. Seven components were used—C_1 through C_6 and C_{7+}—with N_2 lumped with methane and CO_2 lumped with C_2. This seven-component regression is referred to as Regression 1. With no regression, the ZJRK EOS predicted bubblepoint pressures of 2,934 and 2,915 psia [20 229 and 20 098 kPa] for the original nine and lumped seven components, respectively.

Fig. 2 compares calculated and observed expansion data. The poor agreement of volume percent liquid values in the 1,600- to 2,600-psia [11 032- to 17 927-kPa] pressure range reflects, in part, omission of data in this range from the regression data set. (Fig. 9, discussed later, indicates the better agreement obtained when more points of the expansion test are included in the regression.)

Fig. 3 shows the black-oil PVT properties calculated by the material balance method described in Appendix C. The properties are virtually independent of whether they are calculated from the constant-composition expansion or from a constant-volume expansion. The peculiar curve shapes, including the increase of B_g with pressure near dewpoint, are not a consequence of the particular EOS used. The PR and SRK equations, subjected to the same regression, give curves virtually identical to those shown in Fig. 3.

The B_g behavior near dewpoint is a simple consequence of the mass conservation principle. The same behavior is noted regardless of whether B_g is calculated from n-component or from pseudo two-component EOS or material-balance (Appendix C) calculations.

Table 3 gives data for a single-well, one-dimensional (1D) radial, depletion simulation. Formation thickness, permeability, and porosity are 200 ft [60.96 m], 5 md, and 0.25, respectively. Initial reservoir pressure is 4,016 psia [27 689 kPa] with water and gas saturations of 0.2 and 0.8, respectively. Water remains immobile throughout the depletion. The well is flowed on deliverability against a constant bottomhole flowing pressure (BHFP) of 1,250 psia [8618 kPa]. Eight radial gridblocks were used. Results were insensitive to use of more blocks

TABLE 2—REGRESSION DATA SET

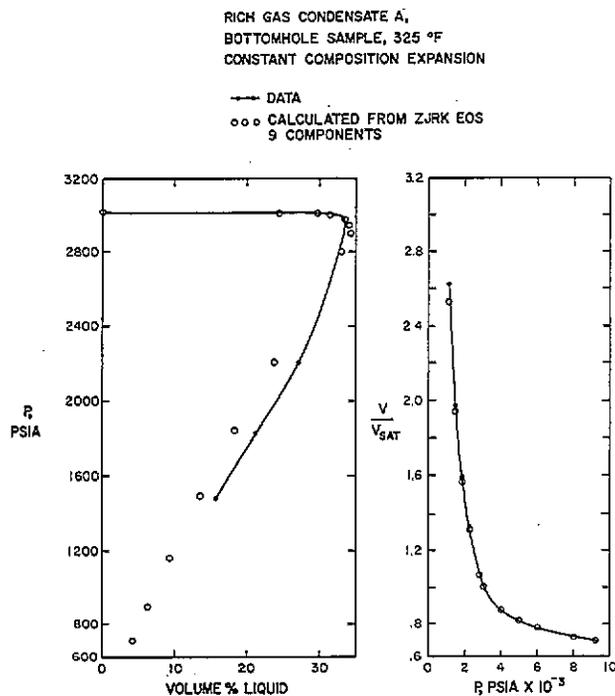|	Data	Calculated After Regression
Dewpoint pressure, psia	3,025	3,025
Gas z-factor at dewpoint	0.7810	0.7810
V/V_s at 1,490 psia	1.9703	1.9365
V/V_s at 7,000 psia	0.7419	0.7419
Volume fraction of liquid at 2,970 psia	0.3349	0.3349
Single-stage GOR, (scf/bbl)	1,706.9	1,706.9
Single-stage gas gravity	0.762	0.786

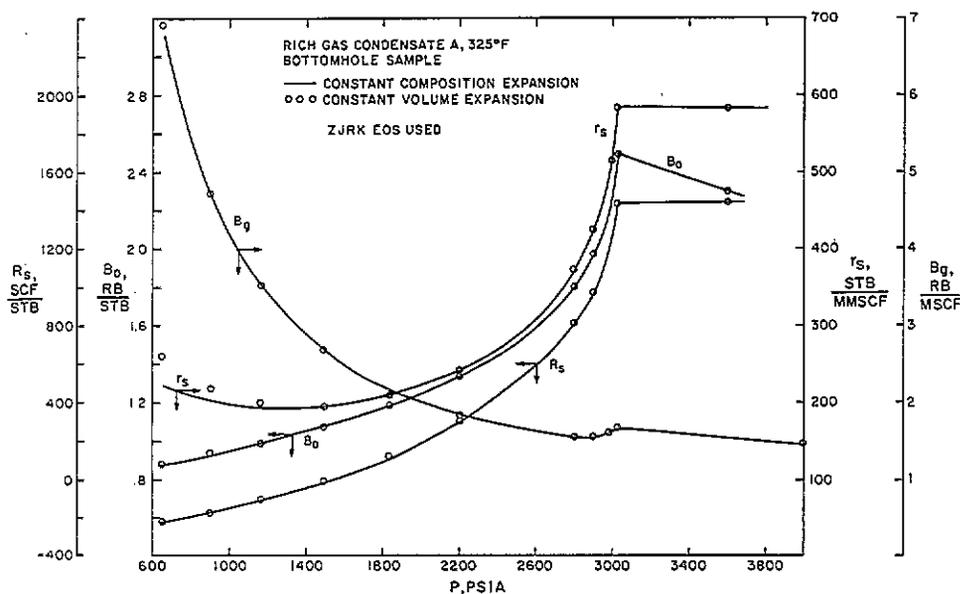Fig. 2—Volume percent liquid and relative volume vs. pressure.

Fig. 3—Calculated black-oil PVT properties.

TABLE 3—RESERVOIR AND FLUID DATA FOR RADIAL SINGLE-WELL SIMULATIONS*

c_w, psi^{-1}	4×10^{-6}
c_r, psi^{-1}	3.5×10^{-6}
Surface gas gravity, air = 1.0	0.7856
Surface oil density, lbm/cu ft	38.91
p_i, psia	4,016
p_s, psia	3,025
P_c	0
S_{wc}	0.2
S_{oi}	0
S_{gi}	0.8
S_{lw}	0.22
S_{orw}	0.3
S_{org}	0.3
k_{rw}	0
k_{rowc}	1.0
k_{rg}	$0.3 \, [S_g/(1 - S_{wc})]^2$
k_{ro}	$[(S_L - S_{wc} - S_{org})/(1 - S_{wc} - S_{org})]^2$, where $S_L = S_w + S_o = 1 - S_g$
h, ft	200
k, md	5
ϕ	0.25
r_w, ft	0.25
Gridblock center radii, ft	4, 8.01, 16.03, 32.1, 64.3, 128.7, 257.7, and 515.9
r_e, ft	744.73
Well productivity index, RB-cp/D-psi	2.55
BHFP, psia	1,250

*Rich-gas Condensate A at 325°F.

and/or a smaller first-block radius. The exterior radius corresponds to a 40-acre [16.19-ha] well spacing.

Fig. 4 shows calculated surface gas production rate (deliverability) and instantaneous producing GOR vs. time. Fig. 5 shows calculated fractional recoveries of gas and oil vs. time. The black-oil (fixed) n-component, surface gas, and oil compositions were read as input data and used to calculate C_{5+} recoveries from the volumetric surface oil and gas production. Fig. 5 compares the calculated C_{5+} recovery vs. time with results by the compositional simulation.

Figs. 4 and 5 indicate very close agreement between black-oil and compositional simulation of rich Condensate A. However, some differences not reflected in those figures are as follows. The surface gas and liquid gravities of the cumulative black-oil production are constant at 0.7856 (air = 1.0) and 0.6235, respectively. The corresponding properties of cumulative gas and oil production in the compositional simulation ranged from 0.7856 and 0.6235, initially, to 0.8072 and 0.6043, respectively, after 8 years. While the C_{5+} recoveries of the two simulations agree well, the distributions within that cut do not. The fractional recoveries of C_5, C_6, and C_{7+} at 8 years were 0.3328, 0.3153, and 0.3031 and 0.4245, 0.3872, and 0.2386 for the black-oil and compositional simulations, respectively.

The difference in component distribution is caused primarily by a significant contribution of mobile liquid flow to total production. Oil-phase relative permeability is zero for oil saturation below 0.3. Calculated oil saturation in the first (near-wellbore) gridblock reached a maximum of 0.423 at 195 days and subsequently declined to 0.36, 0.34, and 0.317 at 700, 1,160, and 2,920 days, respectively. Calculated pressure in the first gridblock was 1,355 psia [9342 kPa] at 2,920 days.

Calculated pressure and liquid saturation profiles vs. time are not shown but are almost identical for the two simulations. The loss in deliverability caused by liquid dropout can be characterized roughly by examination of gas relative permeability. At a near-well oil saturation of 0.32 ($S_w = 0.204$), the gas relative permeability is about 0.108, compared to a value of 0.3 at zero liquid saturation. Thus, on this simple basis, a deliverability factor is 0.108/0.3 (or 0.36), which translates to a reduction in deliverability of 64%.

These rich-gas Condensate A results are presented as the most severe test (of the black-oil approximation) that we have encountered to date. In a number of simulation comparisons for leaner condensates, we have noted similar or better agreement in regard to gas rate and GOR for single-well depletion. However, we did not calculate the C_{5+} or individual component recoveries in those cases.
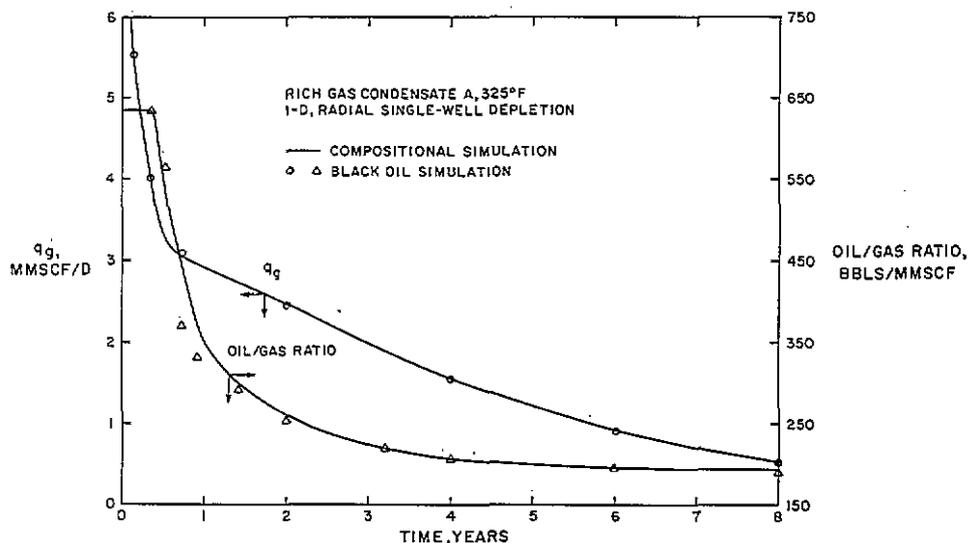

Fig. 4—Comparison of black-oil and compositional simulation results.

TABLE 4—CALCULATED RESULTS FOR CONSTANT-COMPOSITION EXPANSION
Rich-Gas Condensate A, 325°F
(Recombined Sample)

p (psia)	(1) S_L	(2) S_L	(3) S_L	(4) B_g	(5) B_g	(6) ρ_g	(7) γ_L
9,255				0.6339	0.6339		
6,000				0.7337	0.7337		
3,115	0.0	0.0	0.0	1.0148	1.0148	2.7306*	0.6313*
3,100	0.1000	0.1671	0.1671	1.0183	1.0196	2.7328	0.6306
3,017	0.2990	0.2994	0.2999	1.0393	1.0455	2.7396	0.6286
2,992	0.3080	0.3080	0.3085	1.0461	1.0522	2.7412	0.6282
2,905	0.3200	0.3190	0.3197	1.0719	1.0805	2.7459	0.6268
2,660	0.3020	0.3065	0.3074	1.1606	1.1745	2.7570	0.6240
2,385	0.2660	0.2739	0.2749	1.2935	1.3119	2.7682	0.6214
1,792	0.1860	0.1863	0.1876	1.7621	1.7871	2.7912	0.6171

(1) Volume fraction liquid data.
(2) Calculated from PR EOS with nine components.
(3) Calculated from black-oil PVT table, using two pseudocomponent B_g values from PR EOS.
(4) RB wet gas/Mscf wet gas, calculated from PR EOS with nine components.
(5) RB wet gas/Mscf wet gas, calculated from PR EOS with two pseudocomponents.
(6) Density of gas from flash separation of cell gas (from designated pressure) at 624.7 psia, 100°F, lbm/cu ft, calculated from PR EOS with nine components.
(7) Specific gravity of separator liquid at 624.7 psia, 100°F.

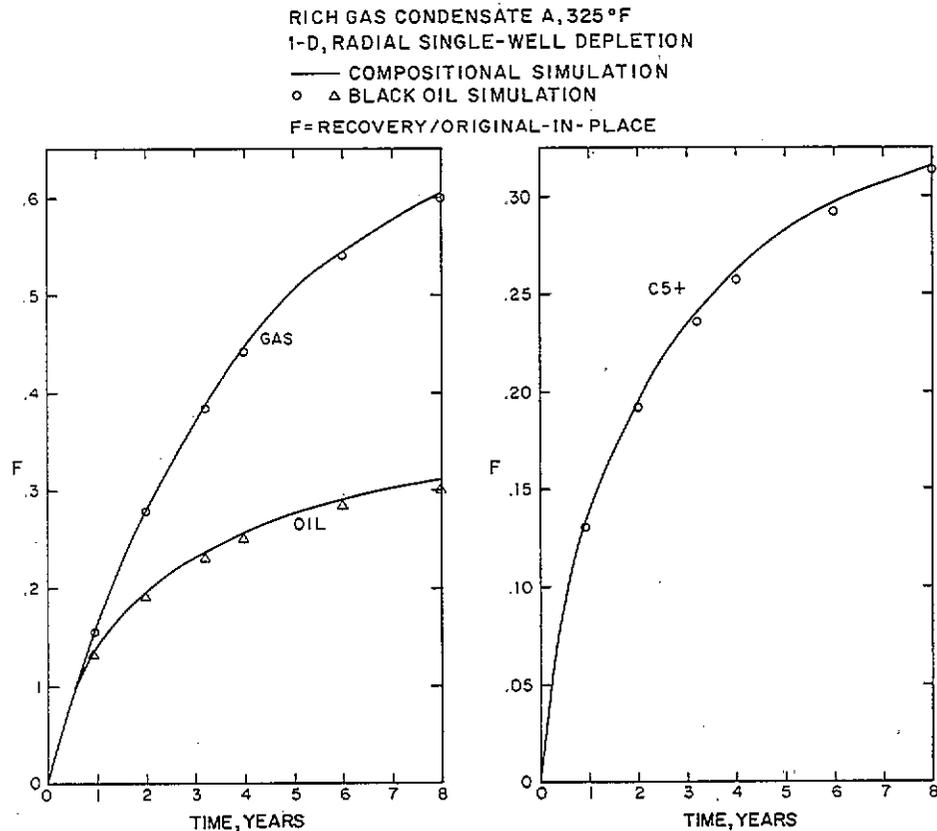*These are fixed densities of (surface) gas and oil used in the black-oil simulator.

RICH GAS CONDENSATE A, 325°F
1-D, RADIAL SINGLE-WELL DEPLETION
——— COMPOSITIONAL SIMULATION
o △ BLACK OIL SIMULATION
F = RECOVERY/ORIGINAL-IN-PLACE

Fig. 5—Comparison of recoveries from black-oil and compositional simulation.

TABLE 5—WELLSTREAM COMPOSITIONS CALCULATED FROM PR EOS AND BLACK-OIL PVT TABLE*

Component	Original Reservoir Fluid	Black-Oil		Wellstream at 1,792 psia	
		Gas	Oil	Black-Oil	Nine-Component EOS
CO_2	0.0201	0.0247	0.0122	0.0219	0.0217
N_2	0.0562	0.0838	0.0091	0.0668	0.0645
C_1	0.4679	0.6883	0.0927	0.5528	0.5418
C_2	0.1265	0.1319	0.1173	0.1286	0.1315
C_3	0.0587	0.0398	0.0909	0.0514	0.0574
C_4	0.0604	0.0207	0.1280	0.0451	0.0544
C_5	0.0392	0.0061	0.0955	0.0265	0.0324
C_6	0.0478	0.0032	0.1237	0.0306	0.0356
C_{7+}	0.1232	0.0014	0.3306	0.0763	0.0608
C_{5+}				0.1334	0.1288

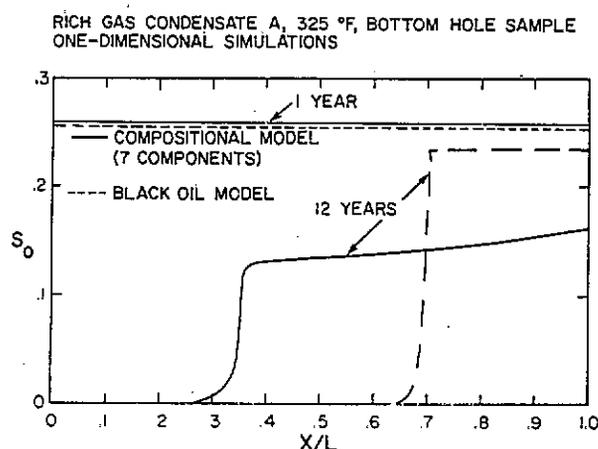*Rich-gas Condensate A at 325°F, recombined sample.

Fig. 6—Calculated oil saturation profiles after 11 years of cycling.

We intend, therefore, no generalization of the Condensate A simulation results related to C_{5+} or component recoveries.

The black-oil PVT representation is based on fixed densities of surface gas and oil. However, the n-component compositional calculations for an expansion yield varying reservoir gas compositions that, on flashing at fixed surface separation conditions, yield varying compositions and densities of surface gas and liquid. We might expect two-component black-oil and n-component compositional simulation results for depletion to differ in some proportion to this variation in surface compositions and densities. Tables 4 and 5 indicate the differences in reservoir liquid dropout and surface densities and compositions resulting from black-oil vs. compositional depletion calculations. Of course, no flow effects are included in these differences.

The nine-component EOS results listed in Tables 4 and 5 were obtained from the PR equation with the original nine components (C_{7+} was not split into fractions). Regression was performed on the recombined sample expansion data. Table 4 shows that the black-oil gas density and the specific gravity of the oil are 2.73 lbm/cu ft [43.73 kg/m^3] and 0.6313 (water=1.0), respectively. The nine-component compositional surface flashing of cell gas from the declining expansion pressures gave gas den-

sity and liquid gravity varying from the latter values at the 3,115-psia [21 477-kPa] dewpoint pressure to 2.7912 lbm/cu ft [44.71 kg/m^3] and 0.6171, respectively, at 1,792 psia [12 355 kPa]. In addition, Table 4 shows the effect of the use of the two-pseudocomponent B_g on calculated liquid dropout. The nine-component and two-pseudocomponent EOS values of B_g are compared directly also.

Table 4 gives black-oil (fixed) surface gas and oil compositions calculated by the PR equation with nine components. These compositions result from flashing the original reservoir fluid at 624.7 psia [4307 kPa] and 100°F [38°C]. Assuming wellstream composition equal to reservoir gas composition allows calculation of the black-oil wellstream composition at any pressure from values of r_s (STB/scf), from surface oil density and molecular weight, and from surface gas and oil (fixed) compositions. Table 5 compares this calculated black-oil wellstream composition at 1,792 psia [12 355 kPa] with the nine-component PR EOS calculated gas composition at the same expansion pressure.

Cycling Calculations

This cycling calculation uses the reservoir and fluid properties given in Tables 1 and 3. The original reservoir fluid is rich-gas Condensate A (bottomhole sample) described with seven components, $C1+N_2$, $C2+CO_2$, C_3 through C_6, and C_{7+}. The horizontal reservoir length, width, and thickness are 933.4, 233.35, and 200 ft [284.5, 71.1, and 60.96 m], respectively. The calculations are 1D and use 20 gridblocks with gas injection into Gridblock 1. Production is from Gridblock 20 on deliverability, against a bottomhole pressure (BHP) of 1,250 psia [8618.4 kPa] with a well productivity index of 0.37 RB-cp/D-psi [8.53×10^{-6} res m^3·Pa·s/d·kPa].

Initial pressure is 3044.2 psia [20 989 kPa] compared to the dewpoint pressure of 3,025 psia [20 857 kPa]. The reservoir is produced for 1 year with no injection. From Years 1 through 12, gas is injected at a constant rate of 400 Mscf/D [11 327 std m^3/d]. This gas is the primary separator (624.7 psia [4307 kPa], 100°F [38°C]) gas of composition (0.7567, 0.1561, 0.0528, 0.0229, 0.0071, 0.0041, and 0.0003), as calculated from the ZJRK EOS after Regression 1 (partially displayed in Fig. 2).

The black-oil simulation was performed with the PVT properties shown in Fig. 3. The compositional model

TABLE 6—COMPONENT DEFINITIONS*

Case 13**	Case 11	Case 9	Case 7	Case 6	Case 9L	Case 5L	Case 4L
CO_2 (0.0253)	CO_2	C_1+N_2	C_1+N_2	C_1+N_2	CO_2	C_1+N_2	C_1+N_2
N_2 (0.0860)	N_2	C_2+CO_2	C_2+CO_2	$C_2+CO_2+C_3+C_4$	N_2	C_2+CO_2	$C_2+CO_2+C_3+C_4$
C_1 (0.6927)	C_1	C_3	C_3+C_4	C_5+C_6	C_1	C_3+C_4	C_5+C_6
C_2 (0.1348)	C_2	C_4	C_5+C_6	F_7	C_2	C_5+C_6	C_{7+}
C_3 (0.0404)	C_3	C_5	F_7	F_8	C_3	C_{7+}	
C_4 (0.0208)	C_4	C_6	F_8	F_9	C_4		
C_5	C_5	F_7	F_9		C_5		
C_6	C_6	F_8			C_6		
C_7	F_7	F_9			C_{7+}		
F_7	F_8						
F_8	F_9						
F_9							
F_{10}							
F_{11}							
Objective Function Attained by Regression							
0.1331	0.1335	0.1325	0.1389	0.1586	0.1326	0.1281	0.1578

*Rich-gas Condensate A, recombined sample.
**Composition of injected cycling gas is given in parentheses.

simulation was derived with the ZJRK EOS with parameters determined in Regression 1. The two models gave calculated oil saturations of about 0.26, average reservoir pressure of about 2,400 psia [16 547 kPa], and a pressure difference (Blocks 1 through 20) of 270 psi [1862 kPa] at the end of 1 year. At the end of 12 years, the black-oil and compositional models showed average reservoir pressures of 1,709 and 1,636 psia [11 783 and 11 280 kPa], respectively, fractional oil recoveries of 0.7194 and 0.6246, respectively, and fractional C_{7+} recoveries of 0.7214 and 0.3942, respectively. Fig. 6 compares calculated oil saturation profiles at Years 1 and 12.

These results clearly indicate the inapplicability of the black-oil model to cycling below dewpoint, at least (or especially) for condensates approaching the richness of Condensate A. In addition, the complete vaporization region calculated by the compositional model casts doubt about the accuracy of that simulation. Cook et al. [12] demonstrated the erroneous vaporization of compositional cycling calculations with lumped C_{7+} fractions. Engineers and researchers have recognized this error for many years.

The remaining calculations described here relate to compositional cycling calculations with different numbers and groupings of components for the recombined sample of Condensate A. Fixed sets of regression data and regression variables were used in all cases. Table 6 defines Cases 13, 11, 9, 7, 6, 9L, 5L, and 4L. The case number reflects the number of components used, and "L" denotes that C_{7+} was retained as a lumped, single component. Case 13 splits C_{7+} into five fractions, while Cases 11 through 6 split the C_{7+} fraction into three components. Pseudoization or lumping of components (defined in Table 6) was performed in accordance with the pseudoization procedure presented in this paper. Fractions F7, F8, and F9 are defined identically for Cases 11, 9, 7, and 6 and differ from the Case 13 Fractions F7, F8, and F9.

The PR EOS was used in all following calculations with the binary interaction coefficients of Katz and Firoozabadi [16] except for CO_2−HC=0.1 and where changed by regression. The regression data for all cases consisted of (1) dewpoint pressure, (2) gas density at dewpoint, (3) constant composition expansion data (see Ta-
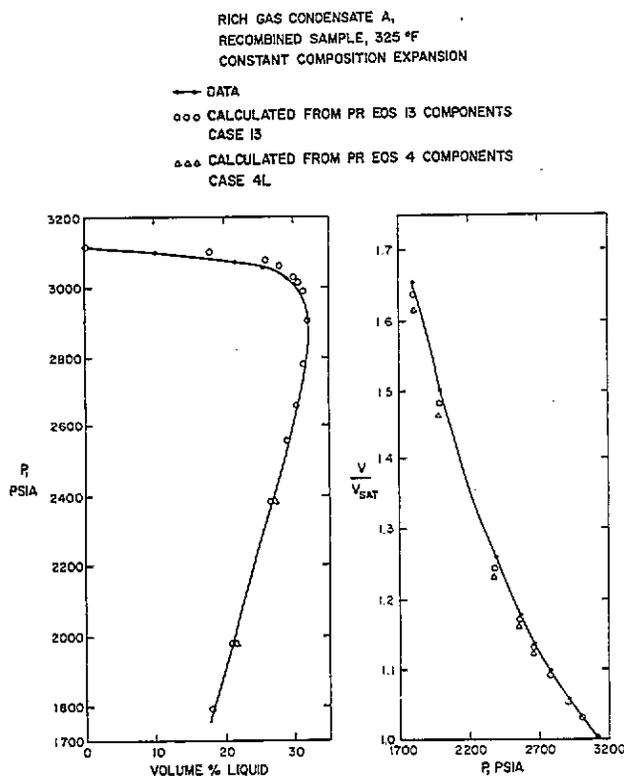

RICH GAS CONDENSATE A,
RECOMBINED SAMPLE, 325 °F
CONSTANT COMPOSITION EXPANSION

DATA
CALCULATED FROM PR EOS 13 COMPONENTS CASE 13
CALCULATED FROM PR EOS 4 COMPONENTS CASE 4L

Fig. 7—Volume percent liquid and relative volume vs. pressure.

ble 1) for points 13, 14, 15, 17, and 20: V/V_S and volume fraction liquid, and (4) GOR and gas gravity for single-stage separation at 624.7 psia [4307 kPa], 100°F [38°C].

The regression variable set for all cases was Ω_a^o and Ω_b^o of C_{7+}, the methane–C_{7+} binary interaction coefficient, and Ω_b^o of methane. In cases where C_{7+} was split, the first three variables were values for all split fractions—e.g., for Case 13 Ω_a^o and Ω_b^o of components 9 through 13 and binary of C_1 vs. Components 9 through 13. (After these calculations were performed, we found better results for this and another condensate with Katz

RICH GAS CONDENSATE A, RECOMBINED SAMPLE
ONE-DIMENSIONAL, COMPOSITIONAL (PR EOS) SIMULATION

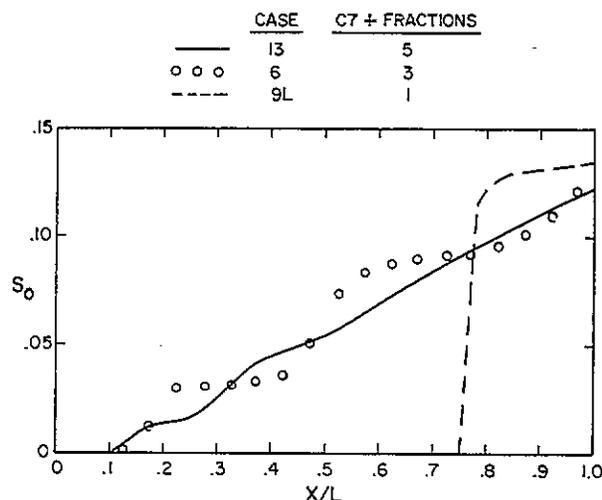|	CASE	C7 + FRACTIONS
——	13	5
o o o	6	3
- - - -	9L	1

Fig. 8—Calculated oil saturation after 11 years of cycling.

TABLE 7—CALCULATED RESERVOIR GAS AND
PRIMARY SEPARATOR GAS DENSITIES AND
VISCOSITIES FOR CASE 13 AT 325°F

	Density (lbm/cu ft)		Viscosity (cp)	
p (psia)	Reservoir Gas	Separator Gas	Reservoir Gas	Separator Gas
6,000	28.1	16.1	0.066	0.033
3,115	20.8	9.2	0.040	0.022
2,555	14.4	7.5	0.027	0.020
1,792	9.2	5.2	0.020	0.018

and Firoozabadi's [16] binaries for all C_1 −HC except the regressed C_1 −F11 [last fraction] binary.)

The agreement between laboratory data and the PR EOS calculations for Case 13 is shown in Fig. 7. The objective function values (see Eq. 7) attained for all cases are listed in Table 6. Calculated results for all cases, except 6 and 4L, plot on Fig. 7 within a fraction less than 1 of symbol size. Case 4L results are shown for points where symbols do not intersect (Fig. 7).

The 1D, horizontal cycling calculations do not reflect gravitational forces or the effects of adverse mobility ratio on conformance. These might be important in above-dewpoint cycling. Calculated reservoir gas and primary separator gas densities and viscosities for Case 13 at 325°F [163°C] are shown in Table 7.

These values indicate that gravity override and adverse-mobility conformance effects might be considerable in above-dewpoint cycling. The values below dewpoint are only of academic interest because of phase equilibration accompanying vaporization during below-dewpoint cycling.

The 1D cycling simulation was performed with the compositional model for all Cases 13 through 4L. The injected gas composition used includes no C_{5+} (Table 6). Tables 8 and 9 show calculated C_{5+} and C_{7+} recoveries vs. time for all cases through 12 years, which corresponds to an injection of 1.9 HCPV's of lean gas.

All simulations resulted in nearly identical oil saturations and average reservoir pressures of about 26% and 2,540 psia [17 513 kPa], respectively, after 1 year of depletion. At the end of 12 years, all cases resulted in average reservoir pressure and a pressure difference of about 1,600 psia [11 032 kPa] and 210 psi [1448 kPa], respectively (Blocks 1 through 20).

Fig. 8 compares calculated oil saturation profiles at 12 years for Cases 13, 6, and 9L. The profiles for Cases 11, 9, and 7 resemble that shown for Case 6. The profiles for Cases 5L and 4L closely resemble that shown for Case 9L.

The "double plateau" character of Case 6 is accompanied by corresponding regions of essentially uniform equilibrium gas and oil compositions. For example, calculated

TABLE 8—CALCULATED C_{5+} AND C_{7+} CYCLING RECOVERIES*

	C_{5+} Recovery Case (Number of Components)							
Time (years)	13	11	9	7	6	9L	5L	4L
1	0.120	0.121	0.121	0.121	0.120	0.124	0.123	0.123
3	0.317	0.317	0.317	0.318	0.314	0.325	0.321	0.318
5	0.502	0.502	0.502	0.503	0.495	0.515	0.507	0.501
8	0.731	0.730	0.731	0.731	0.719	0.744	0.734	0.722
10	0.828	0.830	0.831	0.830	0.816	0.836	0.826	0.813
12	0.872	0.884	0.885	0.883	0.872	0.897	0.868	0.891

	C_{7+} Recovery Case (Number of Components)							
1	0.109	0.109	0.109	0.109	0.108	0.112	0.111	0.110
3	0.274	0.273	0.273	0.273	0.267	0.280	0.274	0.270
5	0.424	0.423	0.423	0.423	0.412	0.433	0.423	0.415
8	0.612	0.610	0.611	0.607	0.590	0.621	0.606	0.589
10	0.715	0.719	0.720	0.716	0.693	0.725	0.707	0.685
12	0.783	0.803	0.803	0.799	0.781	0.823	0.800	0.774

*Rich-gas Condensate A at 325°F, recombined sample. 1D, compositional simulation.

TABLE 9—CALCULATED K VALUES AT 1,792 psia FROM CYCLING SIMULATION—CASE 13*

					Constant-Composition Expansion
Position, x/L	0.2	0.5	0.7	0.9	
Time (years)	8	7	6	5	
HCPV Injected	1.1	0.92	0.74	0.57	
S_o	0.017	0.094	0.196	0.248	
Component					
C_1	3.683	3.31	2.57	2.31	2.304
C_2	1.335	1.31	1.276	1.256	1.256
C_3	0.865	0.872	0.916	0.931	0.934
C_4	0.539	0.561	0.639	0.675	0.677
C_5		0.4	0.465	0.508	0.511
C_6		0.262	0.340	0.383	0.385
F_7		0.185	0.268	0.313	0.315
F_8		0.077	0.133	0.168	0.169
F_9		0.033	0.066	0.092	0.092
F_{10}	0.0070	0.010	0.027	0.041	0.041
F_{11}	0.00068	0.0023	0.0058	0.0074	0.0098

*Rich-gas Condensate A at 325°F, recombined sample.

Case 6 compositions at 12 years, expressed approximately without normalization, are found in Table 10.

Table 8 and Fig. 8 indicate that pseudoization from 13 to 6 components, retaining a splitting of the C_{7+} fraction, results in a moderate to small loss in accuracy of calculated C_{5+} and C_{7+} recoveries vs. time. The tabular results (for Cases 9L, 5L, and 4L) may seem to indicate that use of the single C_{7+} fraction and pseudoization to five or even four components yields larger but acceptable errors in the recoveries. Fig. 8, however, shows that these cases will yield strongly erroneous vaporization and corresponding saturation profiles and will predict erroneously 100% C_{5+} and C_{7+} recoveries at longer simulation time.

The calculated K values for Cases 13 through 4L exhibit a surprising insensitivity to pseudoization or lumping. Pseudocomponent C_1+N_2, C_5+C_6, and C_{7+} K values for Cases 13, 9L, and 4L were calculated as $\Sigma y_i / \Sigma x_i$ from the PR EOS constant composition expansion calculations (after regression). The summation for each case is over all components included in the pseudocomponent. For example, $K_{C_{7+}}$ for Case 13 is $\Sigma y_i / \Sigma x_i$ with summation over Fractions F7 through F11. Fig. 9 shows that these pseudocomponent K values are nearly identical over the entire pressure range (3,115 to 1,792 psia [21 477 to 12 355 kPa]) in spite of pseudoization from 13 components with five split C_{7+} fractions to only four components. Fig. 9 also illustrates the near-criticality of Condensate A.

The expansion calculations show almost no dependence of K values upon composition (that is, calculated equilibrium phase compositions at a given pressure are nearly the same whether obtained by a constant composition or by a constant-volume expansion).

However, the compositional simulation results show a pronounced dependence of K values on composition. Table 9 lists K values at 1,792 psia [12 355 kPa] calculated from the simulation for Case 13. The K values of propane and all heavier components decrease with increased contact by injected gas. Calculated K values for the heaviest components, Fractions F10 and F11, decrease by factors of 6 and 14, respectively.

CONDENSATE A, RECOMBINED
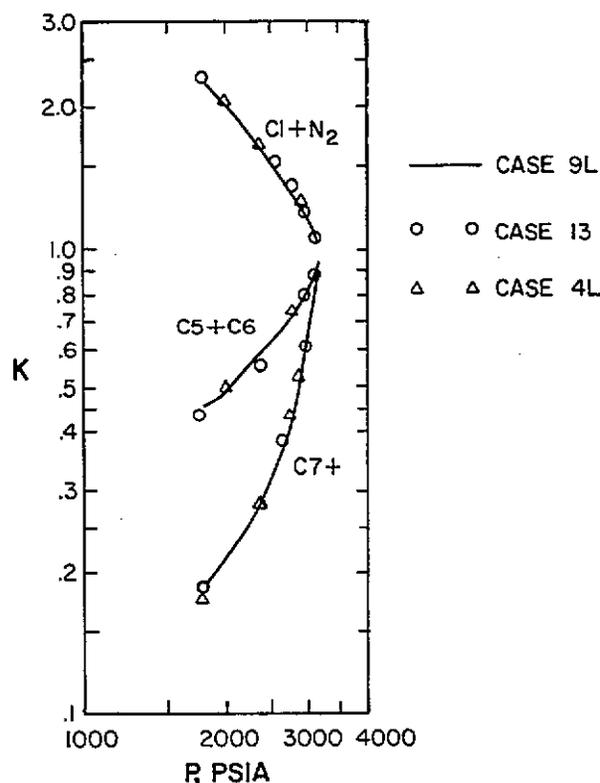SAMPLE 325 °F. PR EOS USED

Fig. 9—Lumped fraction K values calculated from constant composition expansion.

The pseudoization procedure given in this paper does not relate to or preserve any two-phase or saturated mixture properties. It is of some interest, then, to examine the effect of pseudoization alone—with no regression—on EOS-predicted values of saturation pressure and associated properties for Cases 13, 11, 9, 7, 6, 5*, and 4*. Cases 5* and 4* are the same as Case 6 (C_{7+} split into

TABLE 10—CALCULATED COMPOSITIONS FOR CASE 6 AT 12 YEARS

	0.2<x/L<0.45		0.6<x/L<0.85	
Component	Oil	Gas	Oil	Gas
$C_1 + N_2$	0.2	0.78	0.2	0.77
$C_2 + CO_2 + C_3 + C_4$	0.21	0.22	0.207	0.22
$C_5 + C_6$	0	0	0	0
F7	0	0	0	0
F8	0	0	0.44	0.011
F9	0.59	0.0012	0.15	0.0003

Fractions F7, F8, and F9) except that Fractions F8 and F9 are lumped together in Case 5*, and Fractions F7, F8, and F9 are lumped together in Case 4*. Table 11 shows a surprisingly mild variation of saturation properties over this rather pronounced range of pseudoization.

Conclusions

A single form for several widely used cubic EOS's is presented as density (z-factor) and component fugacity equations. This general form stems from manipulation of results given by Martin. [1]

A proposed pseudoization procedure preserves single-phase pseudocomponent and mixture densities and viscosities as functions of pressure and temperature as the number of components describing a mixture is reduced.

This pseudoization procedure and material balance considerations are used to generate two-component, black-oil representations of gas condensates. Black-oil simulations of reservoir depletion for a number of condensates have shown close agreement with results obtained by full compositional modeling. Qualifying this agreement is the fact that we have compared the calculated C_{5+} depletion recoveries only for the near-critical Condensate A discussed in this paper.

Good agreement, in turn, between compositional (EOS) results and experimental laboratory expansion data is shown for Condensate A, provided regression is used.

Full compositional modeling is necessary for accuracy in cycling of condensates below dewpoint. Compositional cycling simulations were performed for the near-critical Condensate A with the number of components ranging from 13 to 4. As noted by other authors, accuracy of calculated vaporization requires a splitting of the C_{7+} into a number of fractions. For this condensate, acceptable accuracy of cycling calculations required a minimal set of about six components, including methane and three to four C_{7+} fractions, with intermediates pseudoized to two or three components.

Nomenclature

b_g = $1/B_g$

b_o = $1/B_o$

B_g = gas formation volume factor, RB/scf [res m³/std m³]

B_o = oil formation volume factor, RB/STB [res m³/stock-tank m³]

c = compressibility, volume/volume-pressure

d_j = regression observation (data) j

f = fugacity, units of pressure

F = objective function value used in regression

h = reservoir thickness, ft [m]

I = total number of regression variables

J = total number of observed data values matched by regressions

k = absolute permeability

k_r = relative permeability

k_{rowc} = relative permeability to oil at connate water and zero gas saturations

K = K value, y/x

L = reservoir length

M = molecular weight

n = number of components in a mixture

N_i = number of mols of component i in a mixture

N_m = total mols of a mixture

p = pressure

P_c = capillary pressure

q = flow rate

r_s = oil vapor in gas, STB/scf [stock-tank m³/std m³]

R = universal gas constant

R_s = solution gas, scf/STB [std m³/stock-tank m³]

S = saturation, fraction

S_{iw} = irreducible water saturation

TABLE 11—EFFECT OF PSEUDOIZATION ON PREDICTED SATURATION PRESSURE AND ASSOCIATED PROPERTIES
Rich-Gas Condensate A, Recombined Sample, 325°F PR EOS Used, No Regression, All p_s Are Bubblepoints

Case*	p_s (psia)	$K_{C_1+N_2}$	$K_{C_5+C_6}$	$K_{C_{7+}}$	z_g	M_g	γ_L	100x μ_g	100x μ_L
13	3,325	1.065	0.909	0.801	0.812	40.8	0.356	3.8	4.4
11	3,378	1.063	0.913	0.807	0.812	41	0.362	3.9	4.5
9	3,357	1.056	0.923	0.826	0.808	41.4	0.361	4.0	4.5
7	3,338	1.054	0.927	0.834	0.805	41.6	0.360	4.0	4.4
6	3,276	1.039	0.947	0.878	0.795	42.5	0.357	4.0	4.4
5**	3,220	1.050	0.932	0.844	0.792	41.9	0.353	3.9	4.3
4†	3,018	1.062	0.916	0.808	0.775	41.5	0.342	3.7	4.2

*Case number = number of components.
**Same as Case 6 except F8 and F9 are lumped together.
†Same as Case 6 except F7, F8, and F9 are lumped together.

S_{org} = residual oil saturation for gas displacement

S_{orw} = residual oil saturation for water displacement

S_{wc} = connate water saturation

t = Martin's[1] volume translation for Eq. A-3

T = temperature, °R unless otherwise stated

v = specific volume, volume/mol

v_i = regression variable i

V = total volume

V/V_S = laboratory cell volume/original cell volume at saturation pressure

W_j = weight factor on regression observation j

x = mol fraction or linear distance

y = mol fraction in a gas phase

z = gas compressibility factor

z_i = mol fraction of component i in Mixture z

γ = specific gravity (air=1.0 for gas, water=1.0 for liquids)

δ_{ij} = binary interaction coefficient between Components i and h

δ^{ij} = binary interaction coefficient between Pseudocomponents i and j

μ = viscosity, cp [Pa·s]

μ^* = viscosity parameter in the Lohrenz et al.[21] correlation

ρ = density, mass/volume

Ψ = fugacity coefficient

ω = acentric factor

Ω_a, Ω_b = EOS constants

Subscripts

B = normal boiling point

c = critical

g = gas

i = component i

j = component j

L = liquid

o = oil

r = reduced (e.g., $p_r = p/p_c$)

w = water

Superscripts

ℓ = Pseudocomponent ℓ

References

1. Martin, J.J.: "Cubic Equations of State—Which?" *Ind. and Eng. Chem. Fund.* (May 1979) 81.
2. Redlich, O. and Kwong, J.N.S.: "On the Thermodynamics of Solutions. V. An Equation of State. Fugacities of Gaseous Solutions," *Chem. Review* (1949) 44, 233.
3. Zudkevitch, D. and Joffe, J.: *AIChE J.* (1970) 16, No. 1, 112.
4. Joffe, J., Schneider, G.M., and Zudkevitch, D.: *AIChE J.* (1970), 16, No. 3, 496.
5. Soave, G.: *Chem. Eng. Sci.* (1972) 27, 1197.
6. Peng, D.-Y. and Robinson, D.B.: "A New Two-Constant Equation of State," *Ind. and Eng. Chem. Fund.* (1976) 15, 59.
7. Fussell, D.D. and Yanosik, John L.: "An Iterative Sequence for Phase Equilibrium Calculations Incorporating the Redlich-Kwong Equation of State," *Soc. Pet. Eng. J.* (June 1978) 173-82.
8. Koval, E.J.: "A Method for Predicting the Performance of Unstable Miscible Displacement in Heterogeneous Media," *Soc. Pet. Eng. J.* (June 1963) 145-54; *Trans.*, AIME, 228.
9. Whitson, C.H. and Torp, S.B.: "Evaluating Constant-Volume Depletion Data," *J. Pet. Tech.* (March 1983) 610-20.
10. Jacoby, R.H. and Yarborough, L.: "PVT Measurements on Petroleum Reservoir Fluids and Their Uses," *Ind. and Eng. Chem.* (Oct. 1967) 59, 48.
11. Fussell, D.D.: "Single-Well Performance Predictions for Gas Condensate Reservoirs," *J. Pet. Tech.* (July 1973) 860-70; *Trans.*, AIME, 255.
12. Cook, A.B., Walker, C.J., and Spencer, G.B.: "Realistic K Values of C_{7+} Hydrocarbons for Calculating Oil Vaporization During Gas Cycling at High Pressures," *J. Pet. Tech.* (July 1969) 901-15; *Trans.*, AIME, 246.
13. Fussell, D.D. and Yarborough, L.: "The Effect of Phase Data on Liquid Recovery During Cycling of a Gas Condensate Reservoir," *Soc. Pet. Eng. J.* (April 1972) 96-102.
14. Whitson, C.H.: "Characterizing Hydrocarbon Plus Fractions," *Soc. Pet. Eng. J.* (Aug. 1983) 683-94.
15. Hoffmann, A.E., Crump, J.S., and Hocott, C.R.: "Equilibrium Constants for a Gas-Condensate System," *Trans.*, AIME (1953) 198, 1-10.
16. Katz, D.L. and Firoozabadi, A.: "Predicting Phase Behavior of Condensate/Crude-Oil Systems Using Methane Interaction Coefficients," *J. Pet. Tech.* (Nov. 1978) 1649-55; *Trans.*, AIME, 265.
17. Patton, J.T., Coats, K.H., and Spence, K.: "Carbon Dioxide Well Stimulation: Part I—A Parametric Study," *J. Pet. Tech.* (Aug. 1982) 1798-1804.
18. Coats, K.H.: "An Equation-of-State Compositional Model," *Soc. Pet. Eng. J.* (Oct. 1980) 363-76.
19. Reid, R.C. and Sherwood, T.K.: *The Properties of Gases and Liquids*, third edition, McGraw-Hill Book Co. Inc., New York City (1977).
20. Abbott, M.M.: "Cubic Equations of State: An Interpretive Review," "Equations of State in Engineering and Research," *Advances in Chemistry Series 182*, Am. Chem. Soc. (1979) Washington, D.C.
21. Lohrenz, J., Bray, B.G., and Clark, C.R.: "Calculating Viscosity of Reservoir Fluids From Their Composition," *J. Pet. Tech.* (Oct. 1964) 1171-76; *Trans.*, AIME, 231.

APPENDIX A

Derivation of a General Form For Cubic EOS's

The well known thermodynamic equations defining fugacity[19] are

$$\ln \Psi \equiv \ln \frac{f}{p} = -\frac{1}{RT} \int_\infty^v \left(p - \frac{RT}{v} \right) dv$$

$$+ z - 1 - \ln z, \quad \dots\dots\dots\dots\dots\dots\dots\dots\text{(A-1)}$$

for a pure component, and

$$\ln \Psi_i \equiv \ln \frac{f_i}{px_i} = -\frac{1}{RT} \int_\infty^V \left(\frac{\partial p}{\partial N_i} - \frac{RT}{V} \right) dV$$

$$- \ln z, \quad \dots\dots\dots\dots\dots\dots\dots\dots\dots\text{(A-2)}$$

for a component in a mixture, where N_i is the mols of component i in the mols of total mixture, N_M. The term Ψ_i is the fugacity coefficient, v is specific volume (volume/mol), V is total volume, and x_i is the mol fraction of component i, N_i/N_M. The compressibility factor z is, by definition, pv/RT.

Martin[1] gives the generalized cubic EOS,

$$p = \frac{RT}{v-t} - \frac{\alpha}{(v-t+\beta)(v-t+\gamma)}. \quad \dots\dots\dots\dots\text{(A-3)}$$

Cursory dimensional analysis shows that t, β and γ must have units of specific volume and that α must have units of (specific volume)^2 times pressure. Abbott[20] invokes the principle of corresponding states in selecting RT_c/p_c as the unit of specific volume. Thus we can express the EOS parameters as

$$t = \Omega_t RT_c/p_c,$$

$$\beta = \Omega_\beta RT_c/p_c,$$

$$\gamma = \Omega_\gamma RT_c/p_c,$$

and

$$\alpha = \Omega_\alpha R^2 T_c^2/p_c, \quad \dots\dots\dots\dots\dots\dots (A\text{-}4)$$

and anticipate that the various dimensionless Ω values are universal constants independent of component identity and temperature. In practice, the Ω values in published EOS's are treated generally as functions of temperature and component identity.

Difficulties in proceeding through detailed derivational steps from Eqs. A-1 through A-4 to Eqs. 2a and 2b are notation and lengthy mechanical manipulations. The "volume translation" t used by Martin in Eq. A-3 is customarily denoted "b" by other authors, while Martin's α is usually denoted "a." Because of the notational confusion, length of the manipulations, and lack of any significant novelty of the result, we will skip the derivational details and simply mention some items that may be helpful to a student or engineer beginning work in this area.

The integration in Eq. A-2 is simplified considerably if the order of differentiation and integration is reversed. For a continuous function $p(x,y)$

$$\int \frac{\partial p(x,y)}{\partial x} dy \equiv \frac{\partial}{\partial x} \int p(x,y)dy, \dots\dots\dots\dots\dots (A\text{-}5)$$

so Eq. A-2 can be written

$$\ln \Psi_i = -\frac{1}{RT} \frac{\partial}{\partial N_i} \int_\infty^V p\,dV + \ln V \Big|_\infty^V - \ln z. \quad \dots (A\text{-}6)$$

When the EOS A-3 is substituted into Eq. A-6, integrated, and then differentiated with respect to N_i, the term on the right side ($\ln V$ at $V=\infty$) cancels out.

Eq. 2a is obtained by dividing Eq. A-3 by p and rearranging it as follows:

$$1 = \frac{1}{z-\tau} - \frac{A}{(z-\tau+B)(z-\tau+C)}, \quad \dots\dots\dots (A\text{-}7)$$

where

$$\tau \equiv tp/RT = \Omega_t p_r/T_r, \quad \dots\dots\dots\dots\dots (A\text{-}8a)$$

$$B = \beta p/RT = \Omega_\beta p_r/T_r, \quad \dots\dots\dots\dots\dots (A\text{-}8b)$$

$$C = \gamma p/RT = \Omega_\gamma p_r/T_r, \quad \dots\dots\dots\dots\dots (A\text{-}8c)$$

and

$$A = \alpha p/R^2 T^2 = \Omega_\alpha p_r/T_r^2. \quad \dots\dots\dots\dots (A\text{-}8d)$$

Rearrangement of Eq. A-7 to a cubic (in z) form, definition of m_1 and m_2 by $B=(1+m_1)\tau$, $C=(1+m_2)\tau$, and relabelling τ as B (not B of Eq. A-8b) gives Eq. 2a.

Mixing rules are required in the integration and differentiation steps of Eq. A-6. The most widely used rules are the following forms:

$$\beta = \sum_{j=1}^n x_j \beta_j$$

or

$$B = \sum_{j=1}^n x_j B_j, \quad \dots\dots\dots\dots\dots\dots\dots (A\text{-}9)$$

for t, β, and γ and a quadratic form

$$\alpha = \sum_{j=1}^n \sum_{\ell=1}^n x_j x_\ell \alpha_{j\ell}$$

or

$$A = \sum_{j=1}^n \sum_{\ell=1}^n x_j x_\ell A_{j\ell}, \quad \dots\dots\dots\dots\dots (A\text{-}10)$$

for α, where $\alpha_{j\ell}$ is usually expressed as $(1-\delta_{j\ell})(\alpha_j \alpha_\ell)^{0.5}$ with the binary interaction coefficient $\delta_{j\ell}$ being symmetric in j and ℓ and $\delta_{jj}=0$.

The manipulations involved in Eq. A-6, then, use

$$\frac{\partial (N_M \beta)}{\partial N_i} = \beta_i \quad \dots\dots\dots\dots\dots\dots (A\text{-}11)$$

and

$$\frac{\partial (N_M^2 \alpha)}{\partial N_i} = 2N_M \sum_{j=1}^n x_j \alpha_{ij}, \quad \dots\dots\dots\dots (A\text{-}12)$$

Because $x_i = N_i/N_M$. Also, simplifications are possible at various stages of Eq. A-6 manipulations if the EOS itself (Eq. A-7) is used. The result of manipulations on Eq. A-6 is Eq. 2b. The first step in Eq. A-6 is, of course, insertion of p from the EOS A-3, written in terms of total mols:

$$p = \frac{N_M RT}{V-N_M t} - \frac{\alpha N_M^2}{(V-N_M t+N_M \beta)(V-N_M t+N_M \gamma)}.$$

$$\dots\dots\dots\dots\dots\dots\dots\dots (A\text{-}13)$$

APPENDIX B

Calculation of Pseudocomponent Properties

The first of the two pseudoization conditions stated in the paper is satisfied by defining pseudocomponent properties as

$$A^\ell \equiv \Omega_a{}^\ell p (T_c{}^\ell)^2 / T^2 p_c{}^\ell$$

$$= \sum_{i=1}^{n} \sum_{j=1}^{n} x_i{}^\ell x_j{}^\ell (1-\delta_{ij})(A_i A_j)^{0.5} \quad \ldots \ldots (B\text{-}1a)$$

and

$$B^\ell \equiv \Omega_b{}^\ell p T_c{}^\ell / T p_c{}^\ell = \sum_{j=1}^{n} x_j{}^\ell B_j, \quad \ldots \ldots \ldots (B\text{-}1b)$$

where

$$p_c{}^\ell = \sum_{j=1}^{n} x_j{}^\ell p_{cj}, \quad \ldots \ldots \ldots \ldots \ldots (B\text{-}2a)$$

$$T_c{}^\ell = \sum_{j=1}^{n} x_j{}^\ell T_{cj}, \quad \ldots \ldots \ldots \ldots \ldots (B\text{-}2b)$$

$$v_c{}^\ell = \sum_{j=1}^{n} x_j{}^\ell v_{cj}, \quad \ldots \ldots \ldots \ldots \ldots (B\text{-}2c)$$

$$M^\ell = \sum_{j=1}^{n} x_j{}^\ell M_j, \quad \ldots \ldots \ldots \ldots \ldots (B\text{-}2d)$$

and

$$\mu^{*\ell} = \sum_{j=1}^{n} (x_j{}^\ell \mu_j^* \sqrt{M_j}) \div \sum_{j=1}^{n} (x_j{}^\ell \sqrt{M_j}), \quad \ldots (B\text{-}2e)$$

where use of the Lohrenz $et\ al.$ [21] viscosity correlation is presumed.

The $\Omega_a{}^\ell$ and $\Omega_b{}^\ell$ given by Eqs. B-1a and B-1b are independent of pressure. They are respectively dependent on temperature if and only if any of the Ω_{ai} and Ω_{bi} are dependent on temperature. Eqs. B-1a through B-2e ensure that the EOS will give identical pseudocomponent density vs. temperature and pressure, whether calculated in one-component or n-component mode. Eqs. B-1a and B-1b are obtained directly from Eqs. 2a through 3e.

Eqs. B-2a through B-2e are obtained by the use of the equations of the Lohrenz $et\ al.$ [21] viscosity correlation—that is, if one-component density and n-component density of the pseudocomponent are identical and one-component properties are defined by Eqs. B-2a through B-2e, then that viscosity correlation will give identical viscosities whether calculated in one- or n-component modes.

The second condition of pseudoization is satisfied by Eqs. B-1a through B-2e, and by the additional require-

ment that for each pair of pseudocomponents, the pseudobinary interaction coefficient is given by

$$\sum_{i=1}^{2} \sum_{j=1}^{2} \alpha_i \alpha_j (1-\delta^{ij})(A^i A^j)^{0.5}$$

$$= \sum_{i=1}^{n} \sum_{j=1}^{n} x_i x_j (1-\delta_{ij})(A_i A_j)^{0.5}. \quad \ldots \ldots (B\text{-}3)$$

The pair of pseudocomponents are arbitrarily labelled Components 1 and 2 on the left side of Eq. B-3. $\{x_i\}$ is the n-component composition of an arbitrary mixture of the two pseudocomponents—i.e.,

$$x_i = \alpha_1 x_i^1 + \alpha_2 x_i^2, \quad \ldots \ldots \ldots \ldots \ldots \ldots (B\text{-}4)$$

where $\alpha_1 + \alpha_2 = 1.0$ and $0 < \alpha_j < 1$ for $j=1$, 2. The values of α_1 and α_2 are arbitrary because they cancel out when the left side of Eq. B-3 is expanded, when Eq. B-4 is substituted into the right side of Eq. B-3, and when Eq. B-1a is used.

The only unknown in Eq. B-3, after use of Eq. B-1a, is δ^{12}—i.e., the pseudobinary interaction coefficient between Pseudocomponents 1 and 2. This coefficient δ^{12} is independent of temperature regardless of temperature dependence of Ω_{ai} and/or Ω_{bi}, provided, of course, that the δ_{ij} are independent of temperature.

APPENDIX C

Calculation of Black-Oil PVT Properties for Gas Condensates

This Appendix describes a calculational procedure for gas condensates that determines a black-oil (two-component, surface gas and oil) PVT table of B_o, R_s, μ_o, c_o, B_g, r_s, and μ_g vs. pressure, which will reproduce, approximately, constant-volume or constant-composition laboratory expansion data.

The EOS PVT program is used first with regression to match dewpoint pressure, available expansion data, and surface separation data. The "calibrated" EOS is used then to perform a specified single- or multistage surface separation. The final-stage products, as indicated in Fig. 1, are referred to hereafter simply as gas and oil, with fixed gas gravity (M_g) and gas and oil densities at final-stage pressure and temperature.

The EOS flash of 1 mol of original reservoir wet gas through the specified separation gives the mols of gas and oil obtained together with their n-component compositions, gas molecular weight, density, and oil density. STB used here denotes barrels of final-stage oil, and scf denotes cubic feet of gas at 14.7 psia [101.4 kPa] and 60°F [15.6°C]. The value of r_s STB/scf at dewpoint pressure is easily calculated from these results.

The EOS calculations start with 1 mol of original wet gas at reservoir temperature T and dewpoint pressure and proceed stepwise to expand the gas through a specified sequence of decreasing pressures. Each expansion step is constant-composition, followed by gas withdrawal before the next pressure decrement if the overall expansion is constant-volume.

For any expansion step from pressure p_1 to lower pressure p_2, mass conservation of gas and oil requires that

$$V_2(b_gS_g+b_oR_sS_o)_2 = V_1(b_gS_g+b_oR_sS_o)_1$$

$$\dotfill \text{(C-1a)}$$

and

$$V_2(b_gr_sS_g+b_oS_o)_2 = V_1(b_gr_sS_g+b_oS_o)_1.$$

$$\dotfill \text{(C-1b)}$$

An additional constraint gives the density of the reservoir oil or liquid at p_2, T as

$$\rho_{o2} = b_{o2}(\rho_{ost}+c_1R_{s2}), \dotfill \text{(C-2)}$$

where

$c_1 = 14.7\, M_g/(10.73\times520\times5.6146)$,
$M_g = $ molecular weight of final stage gas, and
$\rho_{ost} = $ final stage oil density, lbm/cu ft.

Rearranging Eq. C-2 gives

$$(b_oR_s)_2 = -\frac{\rho_{ost}}{c_1}b_{o2} + \frac{\rho_{o2}}{c_2} = \alpha b_{o2} + \beta. \dotfill \text{(C-3)}$$

Substituting $(b_oR_s)_2$ from Eq. C-3 into Eq. C-1a and rearranging terms yields

$$S_gb_g + S_o\alpha b_o = \frac{V_1}{V_2}(b_gS_g+b_oR_sS_o)_1 - S_o\beta$$

$$\dotfill \text{(C-4a)}$$

and

$$S_gr_sb_g + S_ob_o = \frac{V_1}{V_2}(b_gr_sS_g+b_oS_o)_1, \dotfill \text{(C-4b)}$$

where, for clarity, subscript 2 has been dropped on S_g, S_o, b_g, r_s, and b_o.

The EOS is used to perform this expansion and yields values of S_g, S_o, V, and r_s at pressure p_2. The value of r_s is obtained by flashing the equilibrium gas at p_2 through the specified surface separation conditions. Eqs. C-4a and C-4b are solved for the two unknowns b_{g2} and b_{o2}, and R_{s2} is then calculated from Eq. C-3.

Whitson and Torp[9] calculate R_s and b_o by flashing the "reservoir" liquid from each expansion pressure at surface separation conditions. The R_s and b_o calculated here lack that physical meaning; rather, they are simply values that satisfy a mass balance and yield correct reservoir oil density.

Repetition of this calculation for each step of the expansion yields the black-oil PVT table desired. Reservoir oil compressibility c_o is easily calculated from the EOS, and the EOS and viscosity correlation[21] give reservoir oil and gas viscosities vs. pressure.

At this point, the black-oil PVT table can be characterized as follows. Consider two calculated expansions at reservoir temperature, T, each being the constant-composition or constant-volume pressure sequence used in the above calculations. The first calculated expansion uses the EOS in full n-component compositional mode, while the second uses the black-oil PVT table. The two calculations will yield identical S_o (liquid dropout) and reservoir liquid and gas densities and viscosities vs. pressure. In addition, if the expansion is constant-volume, the two calculations will yield identical values of mass of gas removed at each step.

The b_g and μ_g values in the black-oil table could be retained as single-valued functions of pressure as calculated above. However, cycling operations can result in undersaturated gas with dependence of b_g and μ_g upon composition (r_s) in addition to pressure. Therefore, one final approximation is made. We pseudoize the (surface) gas n-component composition to one pseudocomponent and the (surface) oil to a second with the pseudoization procedure decribed in this paper. The black-oil model then ignores the PVT table b_g and μ_g values and calculates them from the EOS and viscosity correlation[21] in pseudo two-component mode.

We have noted a generally small difference between these two-component b_g and μ_g values and the table or n-component EOS values below dewpoint pressure. Above dewpoint pressure, the two-component and n-component b_g and μ_g values are identical functions of pressure and composition (r_s) as a consequence of the pseudoization method.

In Eqs. C-2 and C-3, we use ρ_{o2} values calculated from the EOS rather than experimental values. Assuming a difference, greater accuracy of the black-oil simulation should result from use of experimental values. However, when compositional and black-oil model results are compared, the EOS oil densities should be used.

SI Metric Conversion Factors

bbl	$\times$ 1.589 873	E$-$01	= m^3
cp	$\times$ 1.0*	E$-$03	= Pa·s
ft	$\times$ 3.048*	E$-$01	= m
°F	(°F$-$32)/1.8		= °C
lbm/cu ft	$\times$ 1.601 846	E+01	= kg/m^3
lbm mol	$\times$ 4.535 924	E$-$01	= kmol
psi	$\times$ 6.894 757	E+00	= kPa
scf	$\times$ 2.831 685	E$-$02	= std m^3

*Conversion factor is exact.   **JPT**

TABLE 6

CALCULATED C5+ CYCLING RECOVERIES

RICH GAS CONDENSATE A, 325°F

RECOMBINED SAMPLE

ONE-DIMENSIONAL, COMPOSITIONAL SIMULATION

TIME, YEARS	Case (Number of Components)							
	13	11	9	7	6	9L	5L	4L
1	.120	.121	.121	.121	.120	.124	.123	.123
3	.317	.317	.317	.318	.314	.325	.321	.318
5	.502	.502	.502	.503	.495	.515	.507	.501
8	.731	.730	.731	.731	.719	.744	.734	.722
10	.828	.830	.831	.830	.816	.836	.826	.813
12	.872	.884	.885	.883	.872	.897	.868	.891

TABLE 7

CALCULATED C7+ CYCLING RECOVERIES

RICH GAS CONDENSATE A, 325°F

RECOMBINED SAMPLE

ONE-DIMENSIONAL, COMPOSITIONAL SIMULATION

TIME, YEARS	Case (Number of Components)							
	13	11	9	7	6	9L	5L	4L
1	.109	.109	.109	.109	.108	.112	.111	.110
3	.274	.273	.273	.273	.267	.280	.274	.270
5	.424	.423	.423	.423	.412	.433	.423	.415
8	.612	.610	.611	.607	.590	.621	.606	.589
10	.715	.719	.720	.716	.693	.725	.707	.685
12	.783	.803	.803	.799	.781	.823	.800	.774

TABLE 8

CALCULATED K-VALUES AT 1792 PSIA FROM CYCLING SIMULATION

RICH GAS CONDENSATE A, RECOMBINED SAMPLE, 325°F

CASE 13

POSITION, x/L	.2	.5	.7	.9	
TIME, YEARS	8	7	6	5	
HCPV INJECTED	1.1	.92	.74	.57	CONSTANT
S_o	.017	.094	.196	.248	COMPOSITION
COMPONENT					EXPANSION
C1	3.683	3.31	2.57	2.31	2.304
C2	1.335	1.31	1.276	1.256	1.256
C3	.865	.872	.916	.931	.934
C4	.539	.561	.639	.675	.677
C5		.4	.465	.508	.511
C6		.262	.340	.383	.385
F7		.185	.268	.313	.315
F8		.077	.133	.168	.169
F9		.033	.066	.092	.092
F10	.0070	.010	.027	.041	.041
F11	.00068	.0023	.0058	.0074	.0098

TABLE 9

EFFECT OF PSEUDOIZATION ON PREDICTED
SATURATION PRESSURE AND ASSOCIATED PROPERTIES

RICH GAS CONDENSATE A, RECOMBINED SAMPLE

$325^\circ F$ PR EOS USED, NO REGRESSION

ALL P_{SAT} ARE BUBBLE POINTS

CASE*	P_{SAT}	K_{C1+N2}	K_{C5+C6}	K_{C7+}	Z_g	M_g	γ_L	100 x μ_g	μ_L
13	3325	1.065	.909	.801	.812	40.8	.356	3.8	4.4
11	3378	1.063	.913	.807	.812	41	.362	3.9	4.5
9	3357	1.056	.923	.826	.808	41.4	.361	4.0	4.5
7	3338	1.054	.927	.834	.805	41.6	.360	4.0	4.4
6	3276	1.039	.947	.878	.795	42.5	.357	4.0	4.4
5**	3220	1.050	.932	.844	.792	41.9	.353	3.9	4.3
4***	3018	1.062	.916	.808	.775	41.5	.342	3.7	4.2

*Case Number = Number of Components

**Same as Case 6 Except F8 and F9 Lumped Together

***Same as Case 6 Except F7, F8 and F9 Lumped Together
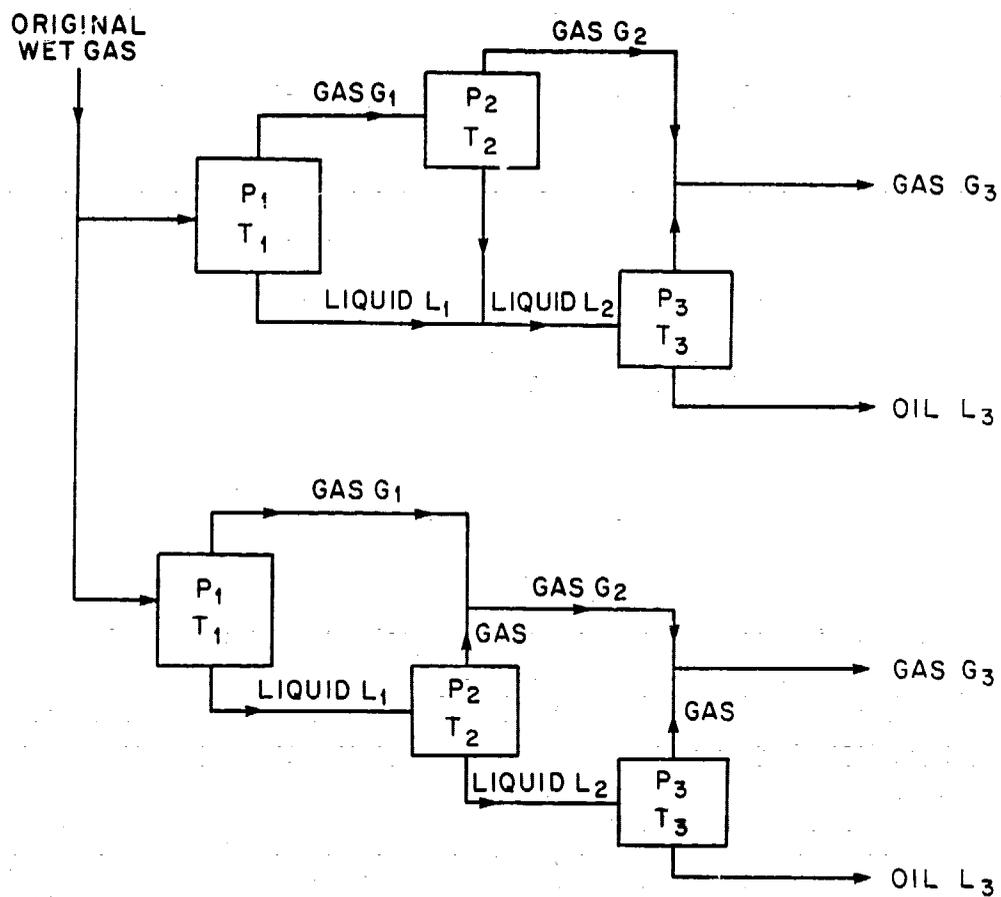
FIGURE 1

EXAMPLES OF GAS CONDENSATE SEPARATION
YIELDING TWO COMPONENTS "OIL" AND "GAS"

RICH GAS CONDENSATE A,
BOTTOMHOLE SAMPLE, 325 °F
CONSTANT COMPOSITION EXPANSION

DATA

o o o CALCULATED FROM ZJRK EOS
9 COMPONENTS
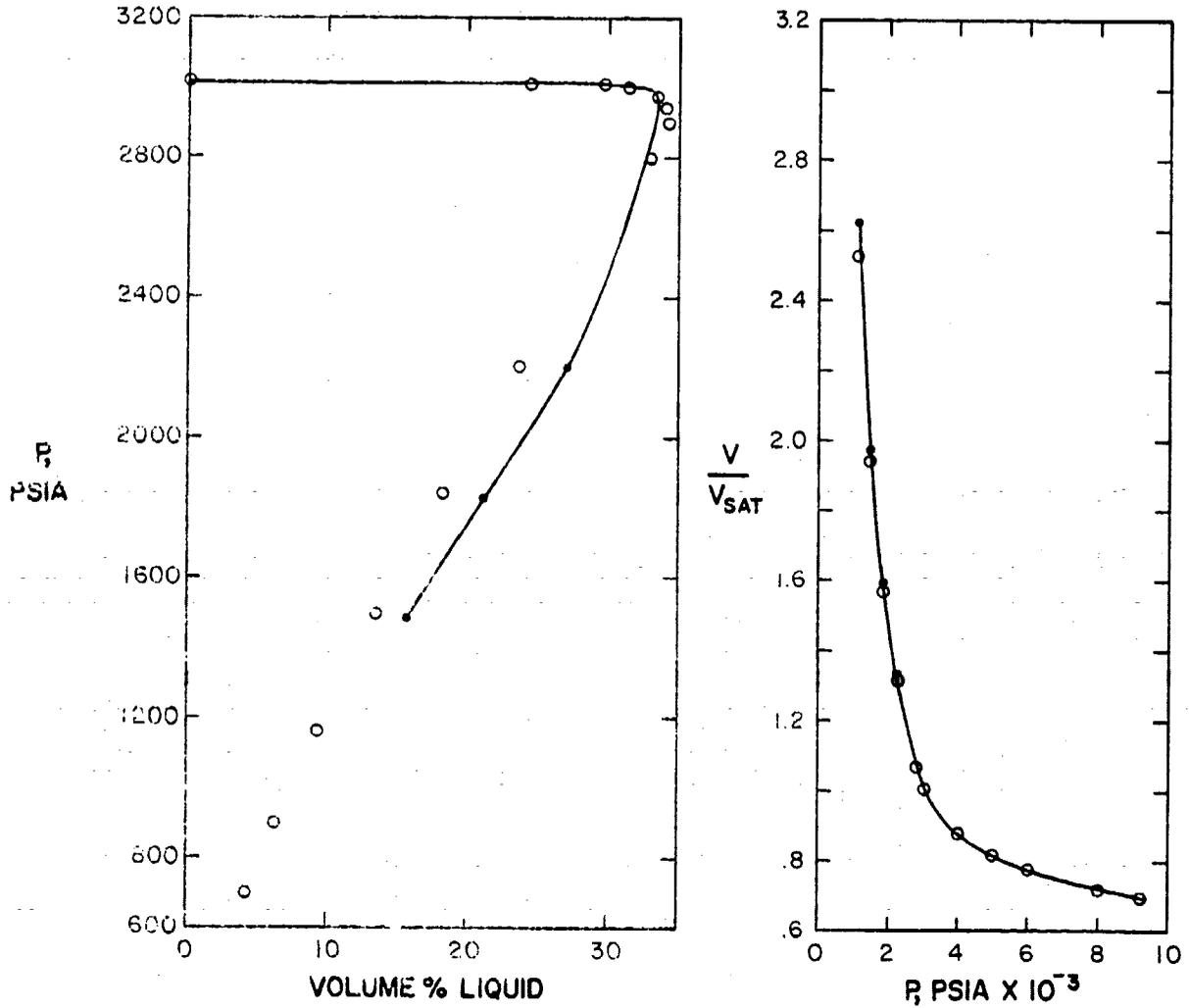
FIGURE 2

VOLUME % LIQUID AND RELATIVE VOLUME vs PRESSURE
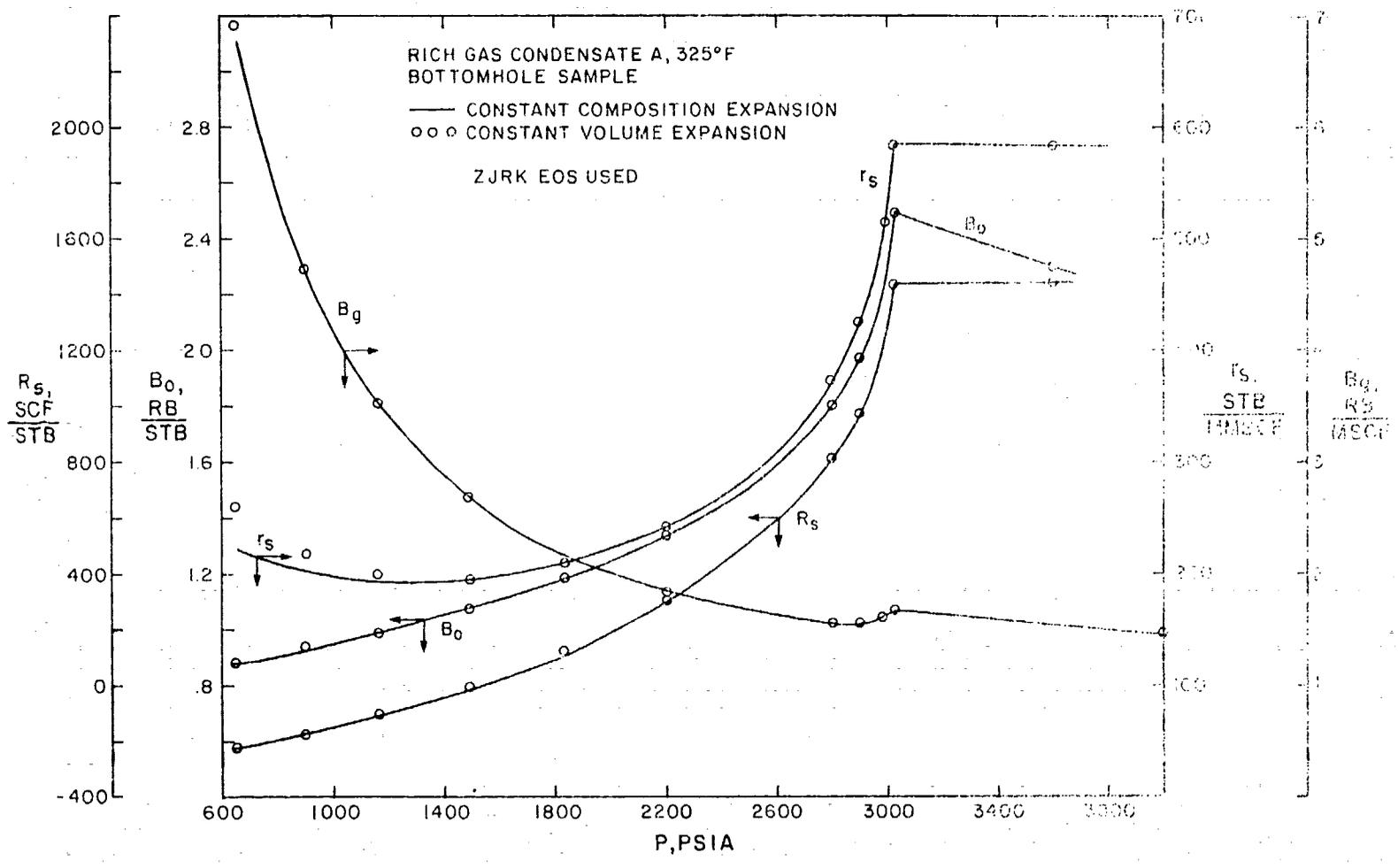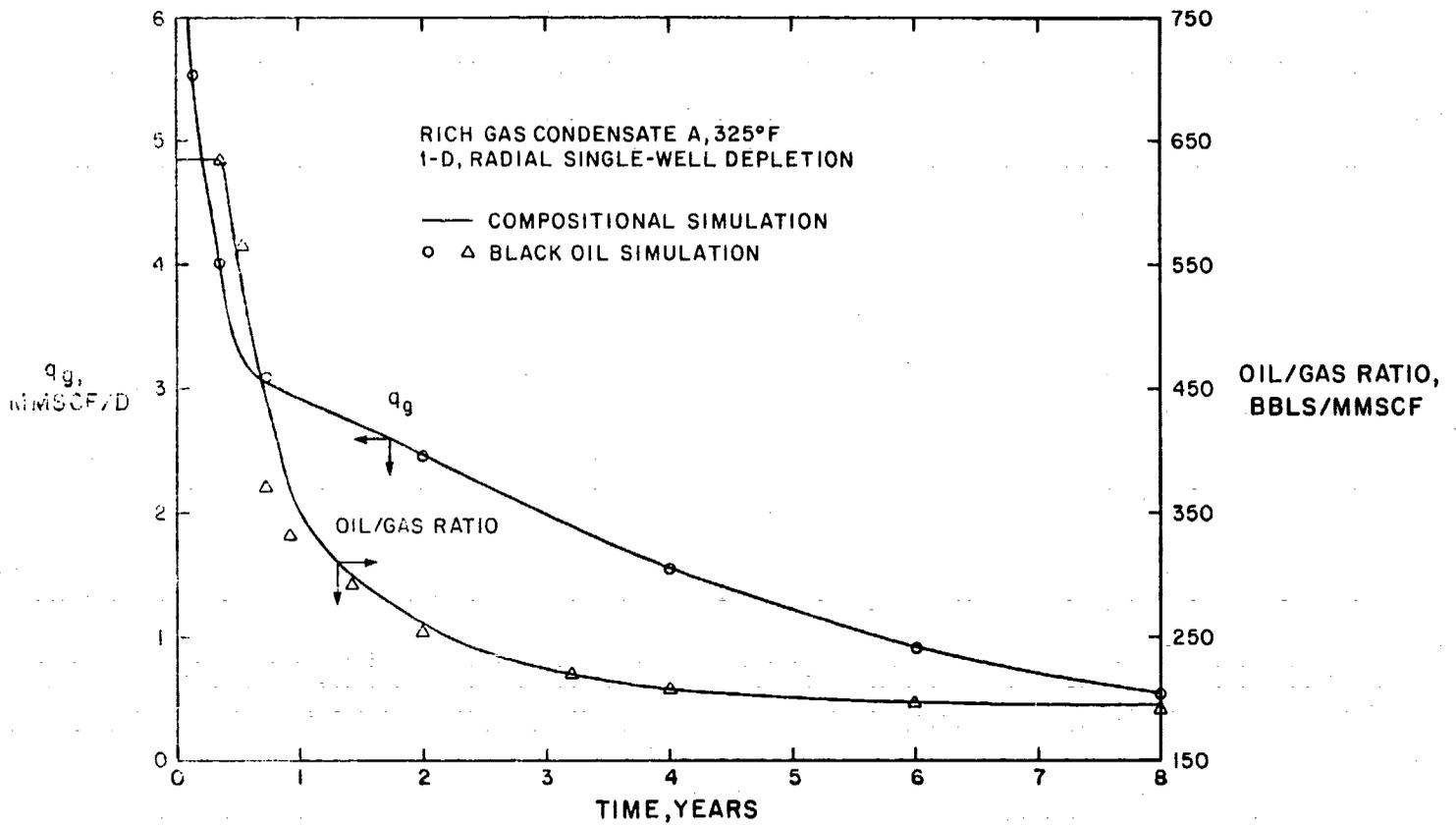
FIGURE 3
CALCULATED BLACK OIL PVT PROPERTIES

FIGURE 4
COMPARISON OF BLACK OIL AND COMPOSITIONAL SIMULATION RESULTS

RICH GAS CONDENSATE A, 325°F
1-D, RADIAL SINGLE-WELL DEPLETION
—— COMPOSITIONAL SIMULATION
o △ BLACK OIL SIMULATION
F = RECOVERY/ORIGINAL-IN-PLACE
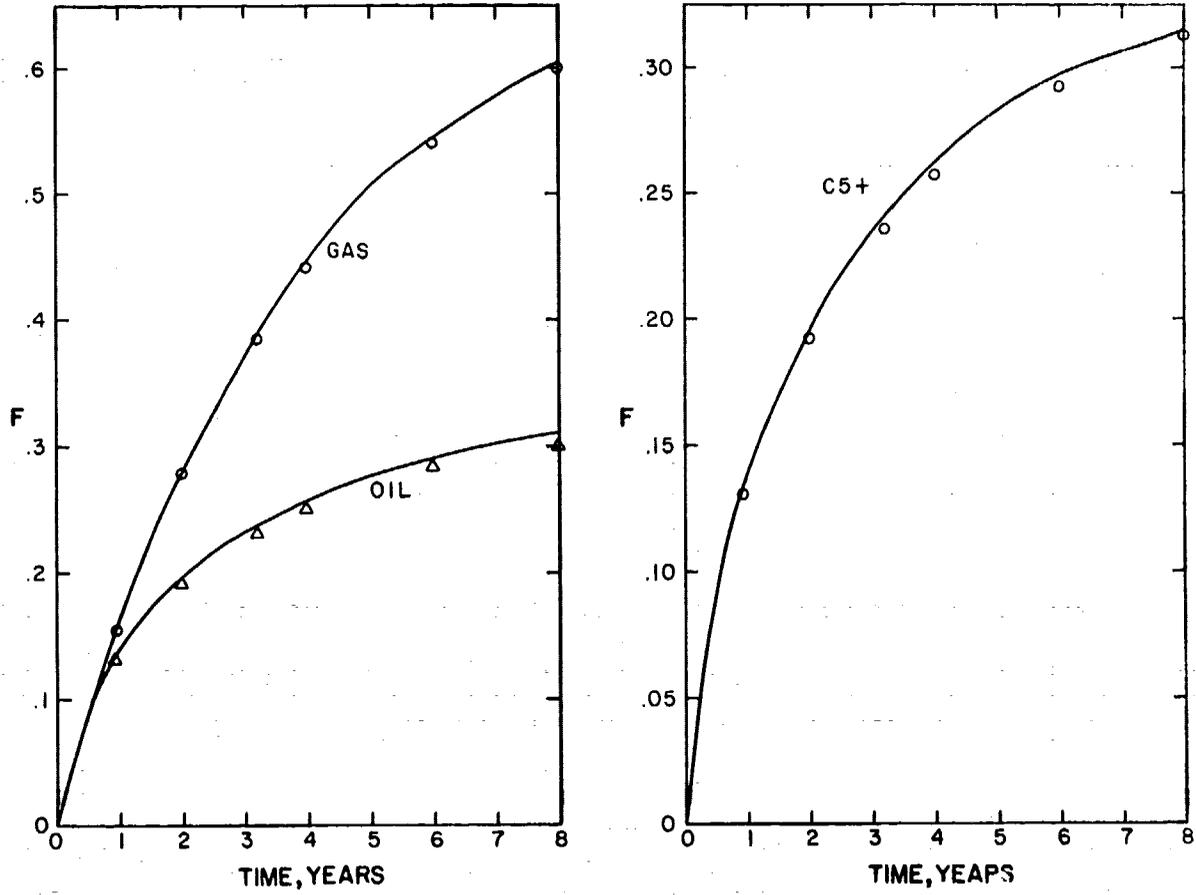
FIGURE 5
COMPARISON OF RECOVERIES FROM BLACK OIL AND
COMPOSITIONAL SIMULATION

CONDENSATE B, 280 °F

—— OBSERVED
ooo CALCULATED FROM PR EOS THIS WORK
●●● CALCULATED FROM ZJRK EOS, THIS WORK
△△△ CALCULATED FROM PR EOS BY WHITSON ET AL (9)
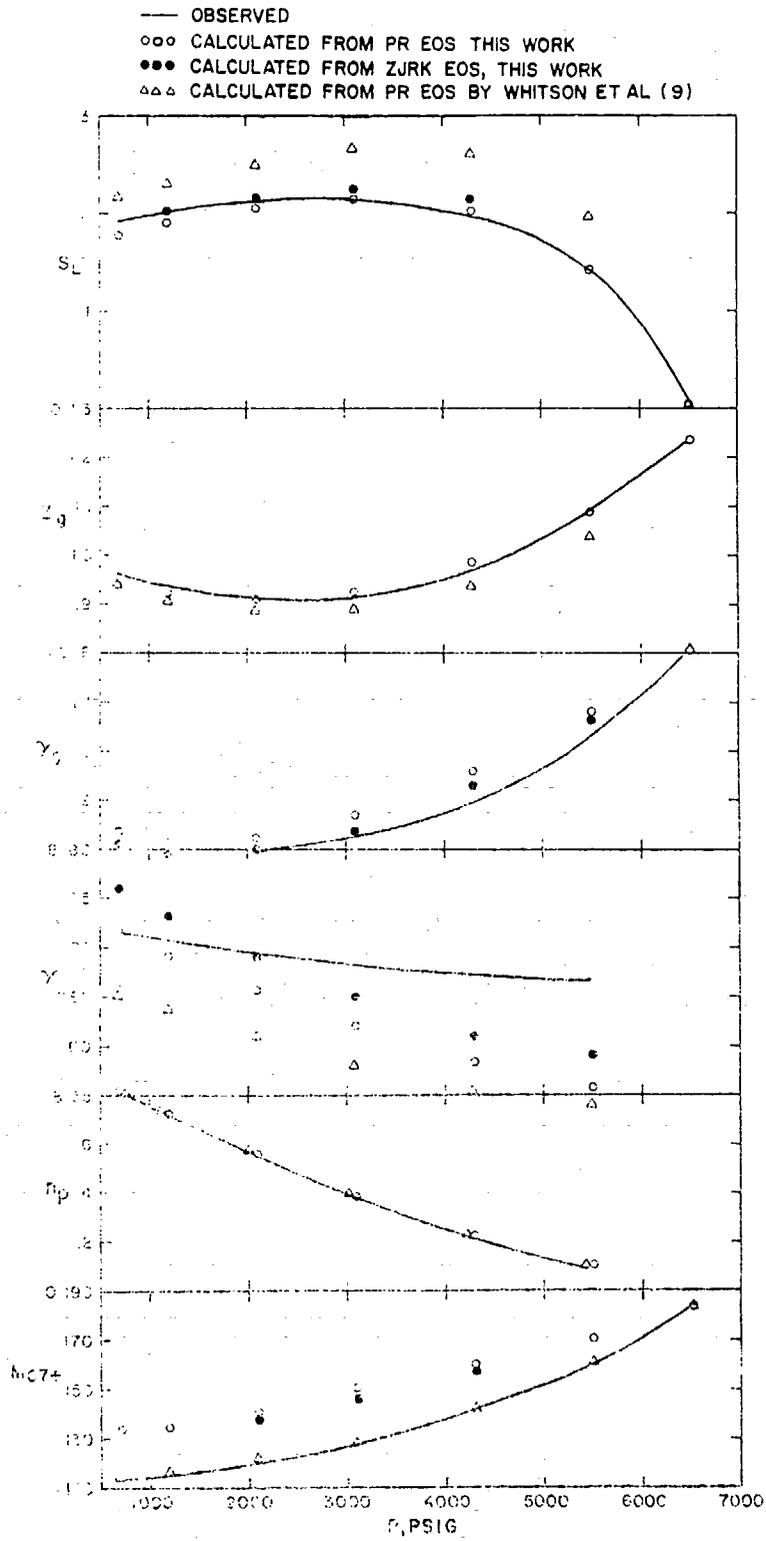
FIGURE 6

CONSTANT VOLUME EXPANSION DATA
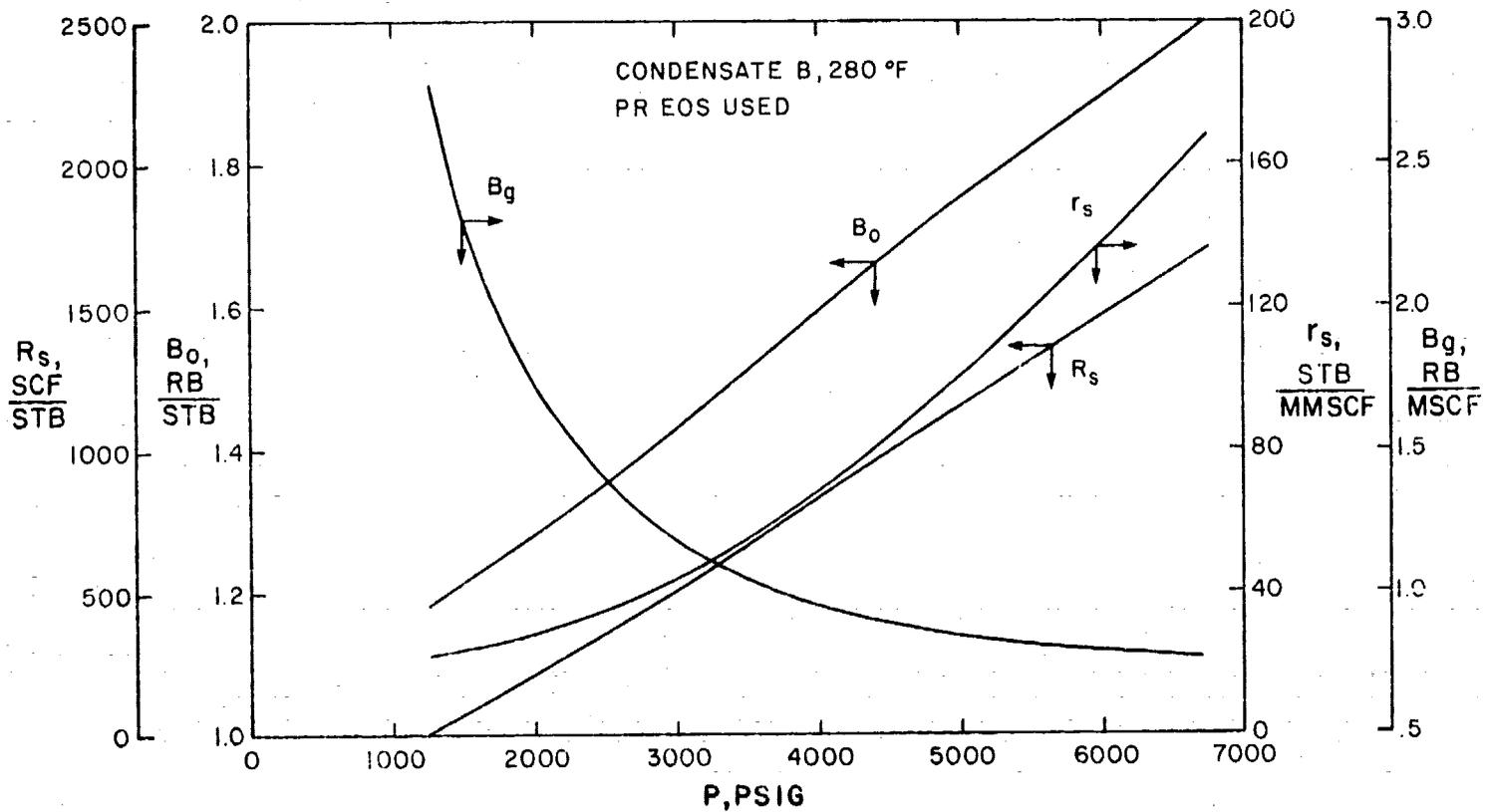
FIGURE 7

CALCULATED BLACK OIL PROPERTIES

RICH GAS CONDENSATE A, 325 °F, BOTTOM HOLE SAMPLE
ONE-DIMENSIONAL SIMULATIONS
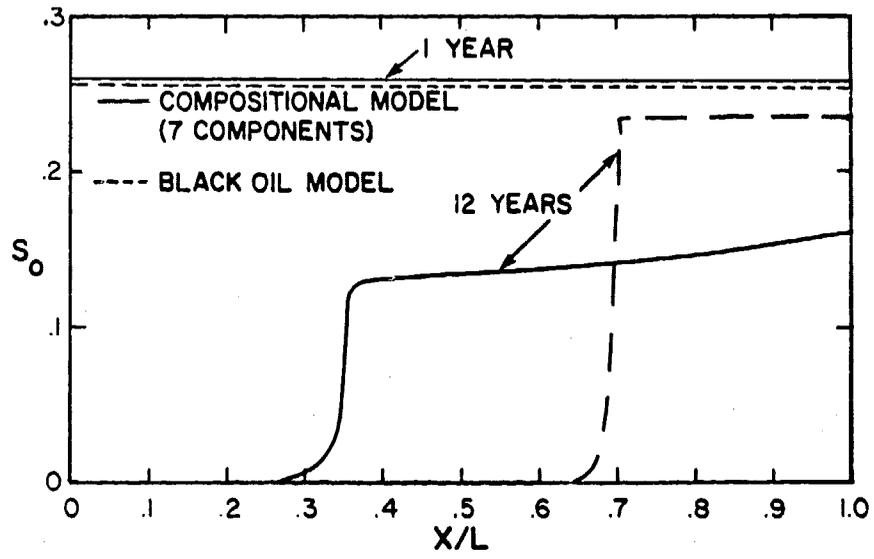
FIGURE 8

CALCULATED OIL SATURATION PROFILES

AFTER 11 YEARS OF CYCLING

RICH GAS CONDENSATE A,
RECOMBINED SAMPLE, 325 °F
CONSTANT COMPOSITION EXPANSION

●—● DATA

ooo CALCULATED FROM PR EOS 13 COMPONENTS
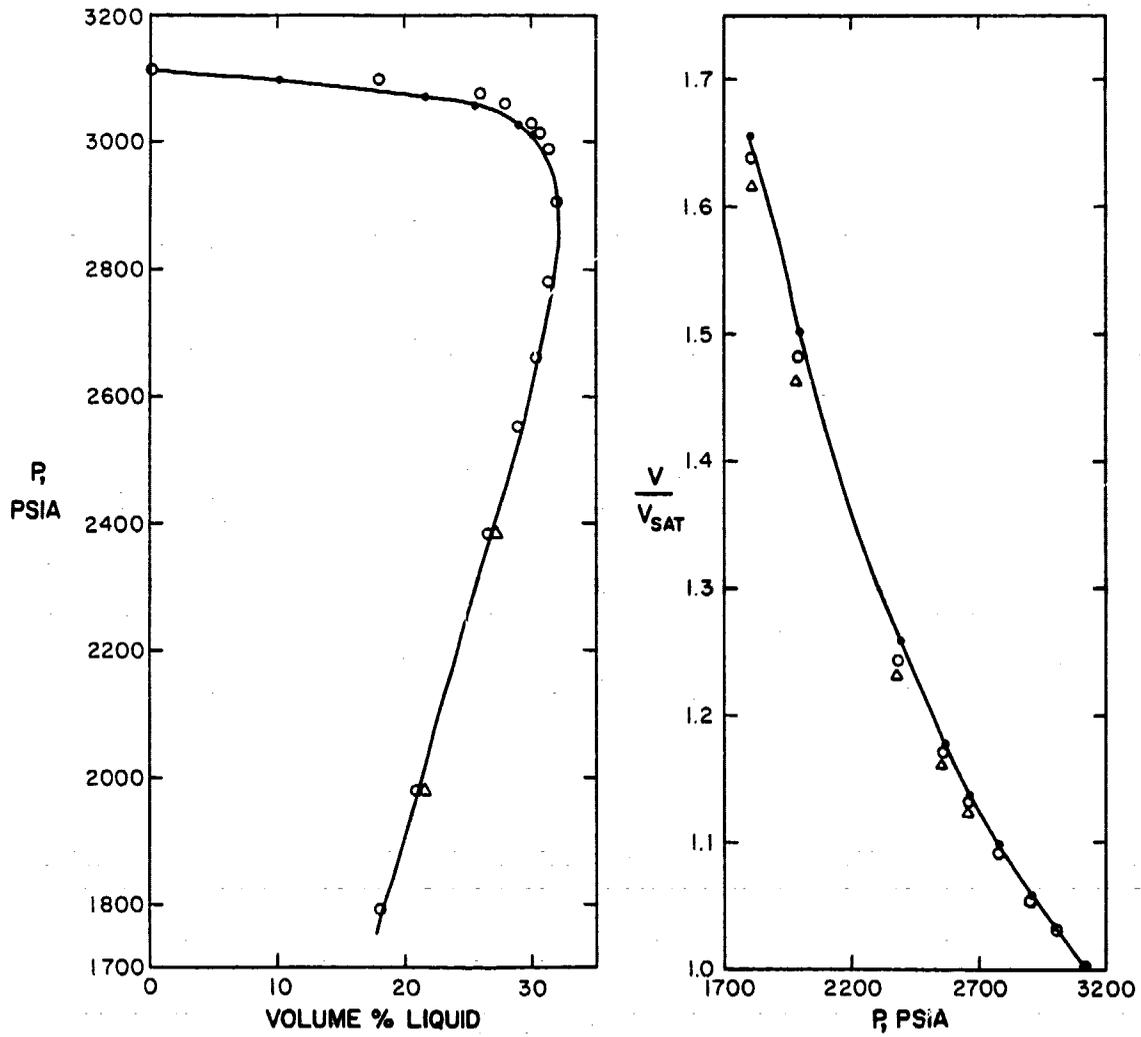CASE 13

△△△ CALCULATED FROM PR EOS 4 COMPONENTS
CASE 4L

FIGURE 9
VOLUME % LIQUID AND RELATIVE VOLUME vs PRESSURE

RICH GAS CONDENSATE A, RECOMBINED SAMPLE
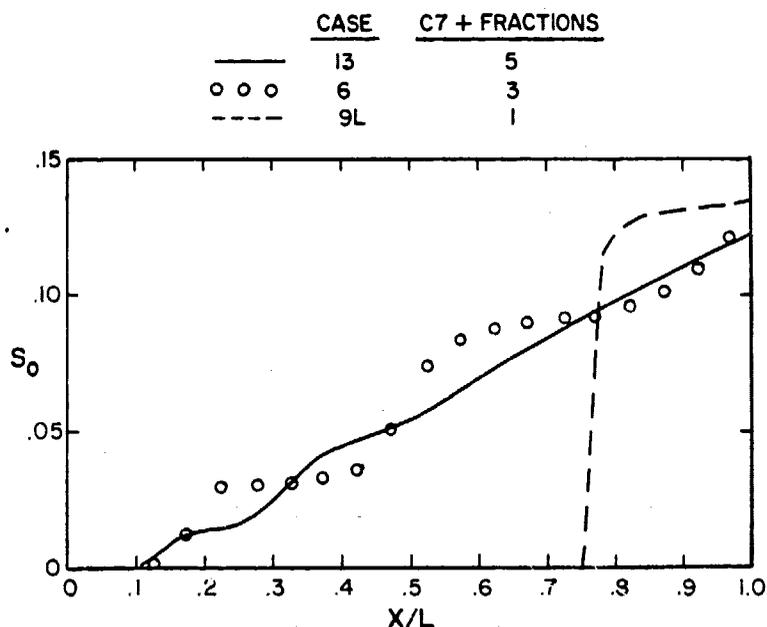ONE-DIMENSIONAL, COMPOSITIONAL (PR EOS) SIMULATION

	CASE	C7 + FRACTIONS
————	13	5
o o o	6	3
– – – –	9L	1

FIGURE 10
CALCULATED OIL SATURATION AFTER 11 YEARS OF CYCLING

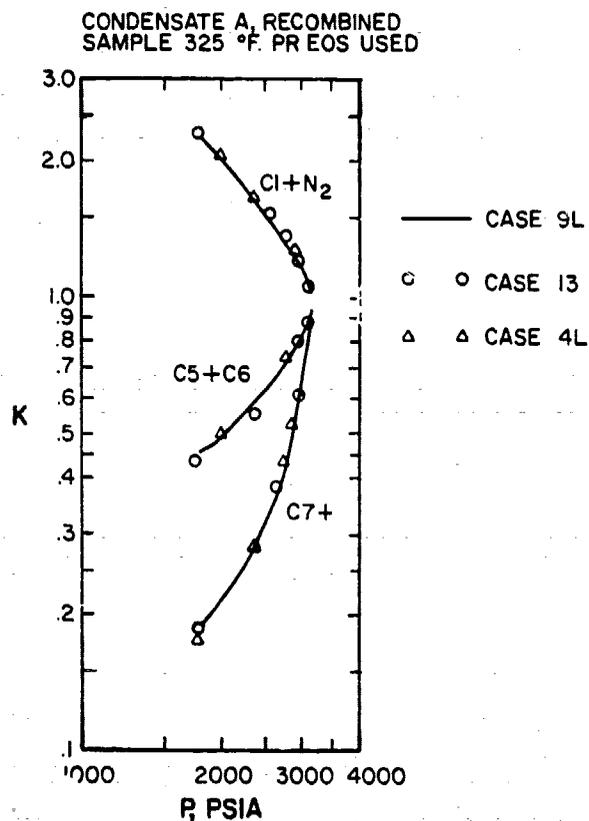CONDENSATE A, RECOMBINED
SAMPLE 325 °F. PR EOS USED

FIGURE 11
LUMPED FRACTION K-VALUES
CALCULATED FROM CONSTANT
COMPOSITION EXPANSION